

A Scalable Graph-Theoretic Distributed Framework for Cooperative Multi-Agent Reinforcement Learning

Gangshan Jing*, He Bai†, Jemin George‡, Aranya Chakrabortty§, and Piyush K. Sharma‡

Abstract

The main challenge of large-scale cooperative multi-agent reinforcement learning (MARL) is two-fold: (i) the RL algorithm is desired to be distributed due to limited resource for each individual agent; (ii) issues on convergence or computational complexity emerge due to the curse of dimensionality. Unfortunately, most of existing distributed RL references only focus on ensuring that the individual policy-seeking process of each agent is based on local information, but fail to solve the scalability issue induced by high dimensions of the state and action spaces when facing large-scale networks. In this paper, we propose a general distributed framework for cooperative MARL by utilizing the structures of graphs involved in this problem. We introduce three graphs in MARL, namely, the coordination graph, the observation graph and the reward graph. Based on these three graphs, and a given communication graph, we propose two distributed RL approaches. The first approach utilizes the inherent decomposability property of the problem itself, whose efficiency depends on the structures of the aforementioned four graphs, and is able to produce a high performance under specific graphical conditions. The second approach provides an approximate solution and is applicable for any graphs. Here the approximation error depends on an artificially designed index. The choice of this index is a trade-off between minimizing the approximation error and reducing the computational complexity. Simulations show that our RL algorithms have a significantly improved scalability to large-scale MASs compared with centralized and consensus-based distributed RL algorithms.

1 Introduction

Traditional Reinforcement Learning (RL) [1] aims to find an optimal policy for a single agent to accomplish a specific task by making this agent interact with the environment. Although RL has found wide practical applications such as board games [2], robotics [3], and power systems [4], the problem is much more complex for multi-agent reinforcement learning (MARL) due to the non-stationary environment for each agent and the curse of dimensionality. MARL, therefore, has attracted increasing attention recently, and has been studied extensively in e.g., [5–17]. The two main challenges of developing distributed cooperative RL algorithms for large-scale multi-agent systems (MASs) are: (i) how to deal with inter-agent couplings all over the network with only local information available for each agent; and (ii) how to guarantee scalability of the designed RL algorithm to large-scale network systems?

Regarding the first challenge, there are mainly three types of inter-agent couplings in MARL that have been considered in the literature, e.g., coupled dynamics (transition probability) [8, 14, 16], partial observations utilized in decision making [6, 10], and coupled reward functions [16]. In [18, 19], all the inter-agent couplings are summarized in one graph, called the coordination graph. The aforementioned references either consider only one type of couplings, or employ only one graph to characterize different types of inter-agent couplings. In fact, the distributed linear quadratic regulator (LQR) design problem

*G. Jing is with School of Automation, Chongqing University, Chongqing 400044, China, jinggangshan@cqu.edu.cn

†H. Bai is with Oklahoma State University, Stillwater, OK 74078, USA. he.bai@okstate.edu

‡J. George and P. Sharma are with the U.S. Army Research Laboratory, Adelphi, MD 20783, USA. {jemin.george,piyush.k.sharma}.civ@mail.mil

§A. Chakrabortty is with North Carolina State University, Raleigh, NC 27695, USA. achakra2@ncsu.edu

involves all the three different inter-agent couplings [20], and distributed RL algorithms have been proposed in the literature to solve this problem, e.g., [21–23]. However, the three types of couplings are not fully utilized in these works. Moreover, the most general formulation of MARL has long been known as the Markov decision process (MDP) [24], while the LQR problem is only a specific application scenario.

The scalability issue, as the second challenge, is resulted from high dimensions of state and action spaces of MAs. Although each agent may represent an independent individual, the inter-agent couplings in the objective function hinder the decomposition of large-size MARL problems. In the literature of distributed RL [5, 8, 10, 25], when dealing with these couplings, the most common method is to make different agents exchange information with each other via a consensus algorithm, so that each agent is able to estimate the value of the global reward function. In this way, the RL algorithm can be designed based on the global information although each agent only has access to local information. However, the performance of such distributed RL algorithms will be similar to or even worse than the centralized RL algorithm because (i) it may take a long time for convergence of consensus when the network is of large scale, (ii) essentially the learning process is conducted via the global reward information. As a result, consensus-based distributed RL algorithms still suffer from significant scalability issues.

In this paper, we develop distributed scalable algorithms for cooperative MARL by utilizing the structures of graphs embedded in the problem. We consider a very general scenario where the dynamics couplings, partial observation relationships and individual rewards couplings may follow different graphs. More specifically, we define *coordination graph*, *observation graph*, and *reward graph*, corresponding to these three types of couplings, respectively. Based on these graphs, we derive a *learning graph*, which describes the required information flow during the RL process. The learning graph also provides a guidance for constructing a local value-function (LVF) for each agent, which is able to play the role of the global value-function (GVF) in learning, but only involves partial agents, and therefore, can enhance scalability of the learning algorithm.

When each agent has access to all the information involved in LVF, distributed RL can be achieved by policy gradient algorithms immediately. However, this approach may require interactions between many agents, which implies a dense communication graph. To further reduce the communication burden, we design a distributed RL algorithm based on local consensus, whose computational complexity depends on the aforementioned three graphs (see Theorem 1). Compared with global consensus-based RL algorithms, local consensus algorithms usually have an improved convergence rate as the network scale is reduced¹. This implies that the scalability of this RL algorithm requires specific conditions on the graphs embedded in the MARL problem. To relax the graphical conditions, we further introduce a truncation index and design a truncated LVF (TLVF), which involves fewer agents than LVF. While being applicable to MARL with any graphs, the distributed RL algorithm based TLVFs only generates an approximate solution, and the approximation error depends on the truncation index to be artificially designed (see Theorem 2). We will show that there is a trade-off between minimizing the approximation error and reducing the computational complexity (enhancing the convergence rate).

In [27], we have considered the case when no couplings exist between the rewards of different individual agents. This paper extends [27] by considering coupled individual rewards, and proposing more detailed relationships between different graphs, distributed RL algorithms via local consensus, and the TLVF-based approach.

The main novel contributions of our work that add to the existing literature are summarized as follows.

- From the formulation perspective, unlike [8, 11], where the global state information is assumed to be known for all agents, we consider a more distributed setting that each agent only has partial observations, whereas both dynamics and rewards of different agents can still be coupled. Although [6, 10, 14, 15] considered partial observations as well, the individual reward of each agent is considered to be independent of other agents in these works. In [16], the inter-agent couplings on both state

¹ Although the convergence rate of a consensus algorithm depends on not only the network scale but also the communication weights, typically the convergence rate can be significantly improved if the network scale is largely reduced. In [26], the relationship between consensus convergence time and the number of nodes in the network is analyzed under a specific setting for the communication weights.

transitions and rewards are considered, but the two graphs are essentially associated with the same graph. In our setting, the three coupling graphs can be fully independent.

- We establish a connection between the coordination graph, the observation graph, the reward graph, the learning graph describing how different agents affect each other, and the communication graph utilized in the learning process. Based on the learning graph, we design a LVF-based distributed policy gradient RL algorithm where only partial agents are involved in gradient estimation. This is different from the policy gradient algorithms based on GVF evaluation in [10, 22]. Although LVFs are designed and employed in [14–16] as well, there is always an approximation error between the partial gradient of each LVF and that of the GVF, which also affects the convergence rate. However, in our work, the partial gradient of each LVF is shown to be exactly the same as that of the GVF, see Lemma 2.
- Our distributed RL algorithm is a policy gradient algorithm based on zeroth-order optimization (ZOO) with exploration in the parameter space. It is known that the dimension of the parameter space is typically higher than that of the action space [28, 29], which is the main shortage of parameter space exploration compared with action-space exploration for RL. In this paper, the sample space dimension for each agent is significantly reduced due to the use of LVFs. Moreover, under different zeroth-order oracles, we show that our learning framework always exhibits a reduced variance of the estimated gradient compared with GVF-based policy evaluation. Note that most of the existing distributed ZOO algorithms [30–33] essentially evaluate policies via GVFs. In [34, 35], LVFs are shown to have reduced variance over GVFs, whereas how to obtain such LVFs in general MARL is not discussed.
- Our second RL algorithm based on TLVF is motivated by [14–16]. Our design, however, is very different from them as we artificially define clusters, and design the TLVF for each cluster by neglecting its effects on other agents that are far away in a coupling graph, whereas in [14–16], each agent has its own TLVF and it is designed by neglecting the effects it receives from agents that are far away in the coupling graph. Moreover, we propose a local consensus approach for each agent to estimate the value of its TLVF.
- A well-studied topic in computer science society called value function factorization or decomposition [18, 19, 36, 37] is very relevant to our work as they aim to find a value function for each agent as well. However, these works directly decomposed the value function approximately according to limited resources available for each agent and were not able to give a reasonable approximation error bound rigorously or establish the relationship between this decomposition and different graphs embedded in the cooperative optimal control problem.

The rest of this paper is organized as follows. Section 2 describes the MARL formulation and the main goal of this paper. Section 3 introduces the LVF design and the learning graph derivation. Section 4 shows the distributed RL algorithm based on LVFs and local consensus, and provides convergence analysis. Section 5 introduces the RL algorithm based on TLVFs as well as the convergence analysis. Section 7 shows several simulation examples to illustrate the advantages of our proposed algorithms. Section 8 concludes the paper.

Notation: Throughout the paper, $\mathcal{G} = (\mathcal{V}, \mathcal{E})$ is an unweighted directed graph, where $\mathcal{V} = \{1, \dots, N\}$ is the set of vertices, $\mathcal{E} \subset \mathcal{V} \times \mathcal{V}$ is the set of edges, $(i, j) \in \mathcal{E}$ means that there is a directional edge in \mathcal{G} from i to j . A path from i to j is a sequence of distinct edges of the form $(i_1, i_2), (i_2, i_3), \dots, (i_{r-1}, i_r)$ where $i_1 = i$ and $i_r = j$. We use $i \xrightarrow{\mathcal{E}} j$ to denote that there is a path from i to j in edge set \mathcal{E} . A subgraph $\mathcal{G}' = (\mathcal{V}', \mathcal{E}')$ with $\mathcal{V}' \subseteq \mathcal{V}$ and $\mathcal{E}' \subseteq \mathcal{E}$ is said to be a strongly connected component (SCC) if there is a path between any two vertices in \mathcal{G}' . One vertex is a special SCC. Given a directed graph $\mathcal{G} = (\mathcal{V}, \mathcal{E})$, we define the *transpose graph* of \mathcal{G} as $\mathcal{G}^\top = (\mathcal{V}, \mathcal{E}^\top)$, where $\mathcal{E}^\top = \{(i, j) \in \mathcal{V} \times \mathcal{V} : (j, i) \in \mathcal{E}\}$. Given two edge sets \mathcal{E}_1 and \mathcal{E}_2 , it can be verified that $\mathcal{E}_1 \subseteq \mathcal{E}_2$ if and only if $\mathcal{E}_1^\top \subseteq \mathcal{E}_2^\top$. Moreover, if $(i, j), (j, i) \in \mathcal{E}$, then $(i, j), (j, i) \in \mathcal{E}^\top$. Given a set A and a vector v , $v_A = (\dots, v_i, \dots)^\top$ with $i \in A$. The

$d \times d$ identity matrix is denoted by I_d , the $a \times b$ zero matrix is denoted by $\mathbf{0}_{a \times b}$. \mathbb{R}^d is the d -dimensional Euclidean space. \mathbb{N} is the set of non-negative integers.

2 Multi-Agent Reinforcement Learning

We model a MARL as a tuple $\mathcal{M} = (\mathcal{V}, \mathcal{E}_C, \mathcal{E}_O, \mathcal{E}_R, \mathcal{E}_{cm}, \Pi_{i \in \mathcal{V}} \mathcal{M}_i, \Pi_{i \in \mathcal{V}} \mathcal{O}_i, \Pi_{i \in \mathcal{V}} r_i, \gamma)$ with $\mathcal{M}_i = (\mathcal{S}_i, \mathcal{A}_i, \mathcal{P}_i)$ specifying the evolution process of agent i , where

- $\mathcal{V} = \{1, \dots, N\}$ is the set of agent indices;
- $\mathcal{E}_C \subseteq \mathcal{V} \times \mathcal{V}$ is the edge set of the *coordination graph* $\mathcal{G}_C = (\mathcal{V}, \mathcal{E}_C)$, which specifies the coordination relationship between agents;
- $\mathcal{E}_O \subseteq \mathcal{V} \times \mathcal{V}$ is the edge set of the *observation graph* $\mathcal{G}_O = (\mathcal{V}, \mathcal{E}_O)$, which determines the partial observation of each agent. More specifically, agent i observes the state of agent j if $(j, i) \in \mathcal{E}_O$;
- $\mathcal{E}_R \subseteq \mathcal{V} \times \mathcal{V}$ is the edge set of the *reward graph* $\mathcal{G}_R = (\mathcal{V}, \mathcal{E}_R)$, which describes inter-agent couplings in the reward of each individual agent;
- $\mathcal{E}_{cm} \subseteq \mathcal{V} \times \mathcal{V}$ is the edge set of the *communication graph* $\mathcal{G}_{cm} = (\mathcal{V}, \mathcal{E}_{cm})$. An edge $(i, j) \in \mathcal{E}_{cm}$ implies that the agent j is able to receive information from agent i ;
- \mathcal{S}_i and \mathcal{A}_i are the state space and the action space of agent i , respectively;
- $\mathcal{P}_i : \Pi_{j \in \mathcal{I}_i^C} \mathcal{S}_j \times \Pi_{j \in \mathcal{I}_i^C} \mathcal{A}_j \times \mathcal{S}_i \rightarrow P(\mathcal{S}_i)$ is the transition probability function specifying the probability of transition to state $s'_i \in \mathcal{S}_i$ under states $\{s_j\}_{j \in \mathcal{I}_i^C}$ and actions $\{a_j\}_{j \in \mathcal{I}_i^C}$, here $\mathcal{I}_i^C = \{j \in \mathcal{V} : (j, i) \in \mathcal{E}_C\} \cup \{i\}$;
- $r_i : \Pi_{j \in \mathcal{I}_i^R} \mathcal{S}_j \times \Pi_{j \in \mathcal{I}_i^R} \mathcal{A}_j \rightarrow \mathbb{R}$ is the immediate reward returned to agent i when each agent $j \in \mathcal{I}_i^R$ takes action $a_j \in \mathcal{A}_j$ at the current state $s_j \in \mathcal{S}_j$, here $\mathcal{I}_i^R = \{j \in \mathcal{V} : (j, i) \in \mathcal{E}_R\} \cup \{i\}$;
- $\mathcal{O}_i = \{\Pi_{j \in \mathcal{I}_i^O} \mathcal{S}_j\}$ is the observation space of agent i , which includes the states of all the agents in \mathcal{I}_i^O , here $\mathcal{I}_i^O = \{j \in \mathcal{V} : (j, i) \in \mathcal{E}_O\} \cup \{i\}$;
- $\gamma \in (0, 1)$ is the discount factor that trades off the instantaneous and future rewards.

Let $\mathcal{S} = \Pi_{j \in \mathcal{V}} \mathcal{S}_j$, $\mathcal{A} = \Pi_{j \in \mathcal{V}} \mathcal{A}_j$, and $\mathcal{P} = \Pi_{j \in \mathcal{V}} \mathcal{P}_j$ denote the the state space, action space and state transition matrix of the whole multi-agent system. Note that the approach proposed in this work is also applicable to the case when \mathcal{P}_i is formulated as a mapping $\Pi_{j \in \mathcal{I}_i^C} \mathcal{S}_j \times \mathcal{A}_i \times \mathcal{S}_i \rightarrow P(\mathcal{S}_i)$, which means that the state of each agent at time step $t + 1$ is only associated with states $s_j(t)$ for $j \in \mathcal{I}_i^C$ and its own action $a_i(t)$. Let $\pi : \Pi_{i \in \mathcal{V}} \mathcal{O}_i \times \mathcal{A} \rightarrow P(\mathcal{A})$ and $\pi_i : \mathcal{O}_i \times \mathcal{A}_i \rightarrow P(\mathcal{A}_i)$ be a global policy function of the MAS and a local policy function of agent i , respectively. Here $P(\mathcal{A})$ and $P(\mathcal{A}_i)$ are the sets of probability measures on \mathcal{A} and \mathcal{A}_i , respectively. The global policy is the policy of the whole MAS from the centralized perspective, thus is based on the global state s . The local policy of agent i is the policy from agent i 's point of view, which is based on o_i composed of partial states. Note that a global policy always corresponds to a collection of local policies uniquely.

At each time step t of the MARL, each agent $i \in \mathcal{V}$ executes an action $a_i(t) \in \mathcal{A}_i$ according to its policy and the local observation $o_i(t) \in \mathcal{O}_i$, then obtains a reward $r_i(s_{\mathcal{I}_i^R}(t), a_{\mathcal{I}_i^R}(t))$. Note that such a formulation is different from that in [8, 11], where the transition and reward of each agent are associated with the global state s_t . Moreover, most of MARL references assume that the reward of each agent only depends on its own state and action. In our work, we consider a more general formulation for cooperative MARL where the reward of each agent may be influenced by other agents, determined by the reward graph $\mathcal{G}_R = (\mathcal{V}, \mathcal{E}_R)$.

The long-term accumulated discounted global reward is defined as

$$R = \sum_{t=0}^{\infty} \gamma^t r(s(t), a(t)) = \sum_{i=1}^N \sum_{t=0}^{\infty} \gamma^t r_i(s_{\mathcal{I}_i^R}(t), a_{\mathcal{I}_i^R}(t)), \quad (1)$$

where $r(s(t), a(t))$ is the global reward for the MAS at time t , r_i is the local reward for agent i at time t . Note that maximizing R is equivalent to maximizing its average $\frac{1}{N}R$, which has been commonly adopted as the learning objective in many MARL references, e.g. [5, 8, 10]. Based on this long term global reward, with a given policy π , we are able to define the global state value-function $V^\pi(s) = \mathbb{E}[\sum_{t=0}^{\infty} \gamma^t r(s(t), a(t))|s(0) = s]$ and state-action value-function $Q^\pi(s, a) = \mathbb{E}[\sum_{t=0}^{\infty} \gamma^t r(s(t), a(t))|s(0) = s, a(0) = a]$, which describe the expected long term global reward when agents have initial state s and initial state-action pair (s, a) , respectively. Similarly, the local state value-function with initial state s' for each agent i can be defined as $V_i^\pi(s) = \mathbb{E}[\sum_{t=0}^{\infty} \gamma^t r_i(s_{\mathcal{I}_i^R}(t), a_{\mathcal{I}_i^R}(t))|s(0) = s]$.

The goal of this paper is to design a distributed RL algorithm for the MAS to find a solution to

$$\max_{\pi} J(\pi) := \mathbb{E}_{s \sim \mathcal{D}} V^\pi(s) = \mathbb{E}_{s \sim \mathcal{D}} \left[\sum_{i=1}^N \sum_{t=0}^{\infty} \mathbb{E}_{a(t) \sim \pi(s(t))} \gamma^t r_i(s_{\mathcal{I}_i^R}(t), a_{\mathcal{I}_i^R}(t))|s(0) = s \right], \quad (2)$$

where \mathcal{D} denotes the distribution that the initial state follow. Our approach is also applicable to other formulations for $J(\pi)$, for example, $J(\pi) = \mathbb{E}_{s \sim \mathcal{D}_s, a \sim \mathcal{D}_a} Q^\pi(s, a)$, where \mathcal{D}_s and \mathcal{D}_a are the two distributions that s_0 and a_0 follow, respectively. Moreover, although we considered maximizing the accumulated rewards along an infinite horizon, the proposed method works for the finite horizon case as well. For convenience of analysis, we also define the expected value to be maximized corresponding to individual reward for each agent i as

$$J_i(\pi) = \mathbb{E}_{s \sim \mathcal{D}} V_i^\pi(s), i \in \mathcal{V}. \quad (3)$$

Note that here J_i may be determined by only the local policies of partial agents, instead of the global policy π . However, the global policy π is always able to determine J_i , therefore, can be employed as the argument of J_i .

We parameterize the global policy $\pi(s, a)$ using parameters $\theta = (\theta_1^\top, \dots, \theta_N^\top)^\top \in \mathbb{R}^d$ with $\theta_i \in \mathbb{R}^{d_i}$. The global policy and agent i 's local policy are then rewritten as $\pi^\theta(s, a)$ and $\pi_i^{\theta_i}(o_i, a_i)$, respectively. Note that given any global state $s \in \mathcal{S}$, a global policy and a collection of local policies can always be transformed to each other. Now we turn to solve the following optimization problem:

$$\max_{\theta} J(\theta) := \mathbb{E}_{s \sim \mathcal{D}} V^{\pi(\theta)}(s), \quad (4)$$

which is an approximation of (2) because the feasible domain of π is restricted to parameterized functions.

Next we give a distributed resource allocation example to demonstrate our formulation.

Example 1 Consider a network of 9 warehouses $\mathcal{V} = \{1, \dots, 9\}$ with a coordination graph $\mathcal{G}_C = (\mathcal{V}, \mathcal{E}_C)$ shown in Fig. 1. The observation graph \mathcal{G}_O only contains 3 edges involving 3 leaf nodes in graph \mathcal{G}_C , as shown in Fig. 1, which implies that only warehouses 2, 3, and 5 observe states of warehouses other than itself. The motivation behind this setting is that warehouses 1, 4 and 6 do not send out resources at all, hence their neighbors need to keep monitoring their states so that the resources sent to them are neither insufficient nor redundant. The reward graph \mathcal{G}_R is shown in Fig. 2, which is the transpose graph of \mathcal{G}_C . This implies that the individual reward of each warehouse involves all of its out-going neighbors in \mathcal{G}_C . Such a setting ensures that each warehouse is responsible for the resource shortages of other warehouses receiving resources from it. At time step t , warehouse $i \in \mathcal{V}$ stores resources of the amount $m_i(t) \in \mathbb{R}$, receives a local demand $d_i(t) \in \mathbb{R}$, sends partial of its resources to and receives resources from its neighbors $j \in \mathcal{N}_i$, besides its neighbors, warehouse i also receives resources of the amount $y_i(t)$ from outside. Let $z_i(t) = y_i(t) - d_i(t)$, then agent i has the following dynamics

$$m_i(t+1) = m_i(t) - \sum_{j \in \mathcal{N}_i^{out}} b_{ij}(o_i(t))m_i(t) + \sum_{j \in \mathcal{N}_i^C} b_{ji}(o_j(t))m_j(t) + z_i(t), \quad (5)$$

$$z_i(t) = A_i \sin(w_i t + \phi_i) + \omega_i,$$

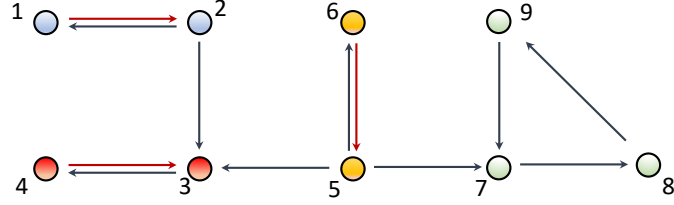


Figure 1: The coordination graph $\mathcal{G}_C = (\mathcal{V}, \mathcal{E}_C)$ and the observation graph $\mathcal{G}_O = (\mathcal{V}, \mathcal{E}_O)$. The black and red lines correspond to edges in \mathcal{E}_C and \mathcal{E}_O , respectively.

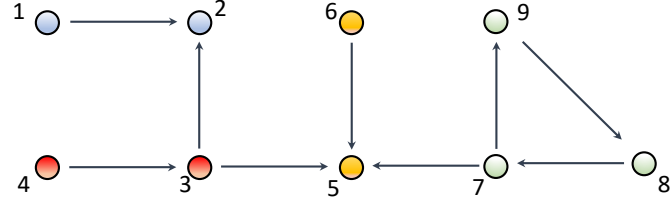


Figure 2: The reward graph $\mathcal{G}_R = (\mathcal{V}, \mathcal{E}_R)$ is the transpose graph of \mathcal{G}_C .

where $b_{ij}(o_i(t)) \in [0, 1]$ denotes the fraction of resources agent i sends to its neighbor j at time t , $0 < A_i < m_i(0)$ is a constant, $w_i, i \in \mathcal{V}$ and $\phi > 0$ are bounded, $\mathcal{N}_i = \{j \in \mathcal{V} : (j, i) \in \mathcal{E}_C\}$ and $\mathcal{N}_i^{out} = \{j \in \mathcal{V} : (i, j) \in \mathcal{E}_C\}$ are the in-neighbor set and the out-neighbor set of agent i , respectively.

From the MARL perspective, besides the three graphs and transition dynamics introduced above, the rest of entries in \mathcal{M} for each agent i at time step t can be recognized as **State**: $s_i(t) = (m_i(t), z_i(t))^\top$. **Action**: $a_i(t) = (\dots, b_{ij}(o_i(t))m_i(t), \dots)_{j \in \mathcal{N}_i^{out}}^\top$. **Individual Policy function**: $\pi_i(o_i(t)) = a_i(t)$. **Partial observation**: $o_i(t) = (\dots, m_j(t), z_j(t), \dots)_{j \in \mathcal{I}_i^O}^\top \in \mathbb{R}^{|\mathcal{I}_i^O|}$. **Individual reward**: $r_i(t) = \sum_{j \in \mathcal{I}_i^R} \tau_j(t)$, where $\tau_j(t) = 0$ if $m_j(t) \geq 0$, and $\tau_j(t) = -m_j^2(t)$ otherwise.

The goal of the resource allocation problem is to maximize $\mathbb{E}_{s(0) \sim \mathcal{D}} \sum_{i=1}^N \sum_{t=0}^{\infty} \gamma^t r_i(t)$ under the dynamics constraint (5). In other words, we aim to find the optimal allocation policy such that each warehouse keeps having enough resources for use.

Remark 1 Note that many settings in this example can be adjusted while maintaining the applicability of the proposed approach in this paper. For example, the partial observation of each agent i can be replaced by $o_i = (\dots, m_j(t), d_j(t), \dots)_{j \in \mathcal{I}_i^O}^\top$ or $o_i = (\dots, m_j(t), \dots)_{j \in \mathcal{I}_i^O}^\top$. Depending on different observation settings, the optimal policy may change.

Existing distributed policy gradient methods such as actor-critic [8] and zeroth-order optimization [10] can be employed to solve the problem when there is a connected undirected communication graph among the agents. However, these approaches are based on estimation of the global value-function, which requires a large amount of communications during each learning episode. Moreover, policy evaluation based on the global value-function has a significant scalability issue due to the high dimension of the state and action spaces for large-scale networks.

3 Local Value-Function and Learning Graph

In this section, we introduce how to design an appropriate LVF for each agent, which involves only partial agents, but its gradient w.r.t. the local policy is the same as that of the global value-function.

3.1 Local Value-Function Design

Although the coordination graph \mathcal{G}_C , the observation graph \mathcal{G}_O , and the reward graph \mathcal{G}_R can be defined independently, we observe that all of them will induce the couplings between different agents in the optimization objective. In this subsection, we will build a connection between these graphs and the couplings between agents, based on which the LVFs will be designed.

Define a new graph $\mathcal{G}_{CO} = (\mathcal{V}, \mathcal{E}_{CO})$ where $\mathcal{E}_{CO} = \mathcal{E}_C \cup \mathcal{E}_O$. Let

$$\mathcal{N}_i^{CO+} = \{j \in \mathcal{V} : i \xrightarrow{\mathcal{E}_{CO}} j\}$$

be the set of vertices in graph \mathcal{G}_{CO} that are reachable from vertex i . Denote $\mathcal{I}_i^{CO+} = \mathcal{N}_i^{CO+} \cup \{i\}$.

Define the following composite reward for agent i :

$$\hat{r}_i(s(t), a(t)) = \sum_{j \in \mathcal{I}_i^L} r_j(s_{\mathcal{I}_j^R}(t), a_{\mathcal{I}_j^R}(t)), \quad (6)$$

where

$$\mathcal{I}_i^L = \{j \in \mathcal{V} : \mathcal{I}_j^R \cap \mathcal{I}_i^{CO+} \neq \emptyset\} = \cup_{j \in \mathcal{I}_i^{CO+}} \mathcal{I}_j^R. \quad (7)$$

Accordingly, we define a LVF for agent i :

$$\hat{V}_i^\pi(s) = \mathbb{E} \left[\sum_{t=0}^{\infty} \gamma^t \hat{r}_i(s(t), a(t)) | s(0) = s \right]. \quad (8)$$

Then agent i is expected to maximize the following objective:

$$\hat{J}_i(\theta) = \mathbb{E}_{s \sim \mathcal{D}} \hat{V}_i^{\pi(\theta)}(s) = \sum_{j \in \mathcal{I}_i^L} J_j(\theta). \quad (9)$$

Different from the global value-function $J(\theta) = \sum_{j \in \mathcal{V}} J_j(\theta)$, the LVF $\hat{J}_i(\theta)$ only involves agents in a subset $\mathcal{I}_i^L \subseteq \mathcal{V}$. We make the following assumption on the graphs so that $\mathcal{I}_i^L \neq \mathcal{V}$ for at least one agent i .

Assumption 1 *There exists a vertex $i \in \mathcal{V}$ such that $\mathcal{I}_i^L \neq \mathcal{V}$.*

Define graph $\mathcal{G}_{COR} = \mathcal{G}_{CO} \cup \mathcal{G}_R^\top$. The following lemma shows a sufficient graphical condition and a necessary graphical condition for Assumption 1.

Lemma 1 *The following statements are true:*

- (i). *Assumption 1 holds if graph \mathcal{G}_{COR} has $n > 1$ SCCs.*
- (ii). *Assumption 1 holds only if graph \mathcal{G}_{CO} has $n > 1$ SCCs.*

Proof: The second statement is straightforward due to the definition of \mathcal{I}_i^L . Next we prove the first one.

Without loss of generality, let i and j be two vertices such that j is not reachable from i in \mathcal{G}_{COR} . Suppose that $\mathcal{I}_i^L = \mathcal{V}$, then there must exist $k \in \mathcal{V}$ such that $j \in \mathcal{I}_k^R$, and $k \in \mathcal{I}_i^{CO+}$. That is, $(k, j) \in \mathcal{E}_R^\top$, implying that j is reachable from i in $\mathcal{G}_{CO} \cup \mathcal{G}_R^\top$, which is a contradiction. \square

One may question if the converse of Lemma 1 is true. The answer is no. This is because graph \mathcal{G}_R^\top may contain some edges that connect different SCCs in \mathcal{G}_{CO} . For statement (i), \mathcal{G}_{COR} may be strongly connected even when there exists a vertex $j \in \mathcal{V} \setminus \mathcal{I}_i^L$. Fig. 3 shows a counter-example where $\mathcal{I}_1^L = \{1, 2\}$ is only a subset of \mathcal{V} but \mathcal{G}_{COR} is strongly connected. For statement (ii), a simple counter-example can be obtained by setting $\mathcal{E}_R = \mathcal{V} \times \mathcal{V}$.

Next we show that each agent $i \in \mathcal{V}$ maximizing its LVF (9) is equivalent to maximizing the global value function (4).

Given a function $f(\theta) : \mathbb{R}^d \rightarrow \mathbb{R}$ and a positive δ , we define

$$f^\delta(\theta) = \mathbb{E}[f(\theta + \delta u)], \quad u \sim \mathcal{N}(0, I_d). \quad (10)$$

The following lemma shows the equivalence between the smoothed LVF $\hat{J}_i^\delta(\theta)$ and the smoothed global value-function $J^\delta(\theta)$.

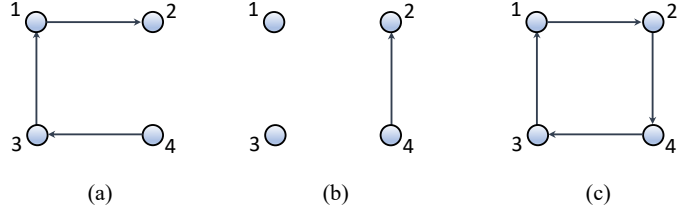


Figure 3: A counter-example for the converse of Lemma 1 (i). (a), (b) and (c) denote graphs \mathcal{G}_{CO} , \mathcal{G}_R , and the resulting \mathcal{G}_{COR} , respectively.

Lemma 2 *The following statements are true:*

- (i) $\nabla_{\theta_i} J^\delta(\theta) = \nabla_{\theta_i} \hat{J}_i^\delta(\theta)$ for any $\delta > 0$, $i \in \mathcal{V}$.
- (ii) If $J_i(\theta)$, $i \in \mathcal{V}$ are differentiable, then $\nabla_{\theta_i} J(\theta) = \nabla_{\theta_i} \hat{J}_i(\theta)$, $i \in \mathcal{V}$.

Lemma 2 reveals the implicit connection between graphs and the couplings between agents in the optimization objective. It is important to note that statement (i) in Lemma 2 does not require $J_i(\theta)$, $i \in \mathcal{V}$ to be differentiable because $J^\delta(\theta) = \mathbb{E}[J(\theta + \delta u)]$ is always differentiable. In order to adapt our approach to the scenario when $J(\theta)$ is not differentiable, we choose to find the stationary point of $J^\delta(\theta)$. The gap between $J(\theta)$ and $J^\delta(\theta)$ can be bounded if $J(\theta)$ is Lipschitz continuous and $\delta > 0$ is sufficiently small.

To guarantee the Lipschitz continuity of $J(\theta)$, we make the following assumption on functions $V_i^{\pi(\theta)}(\theta)$ for $i \in \mathcal{V}$:

Assumption 2 $V_i^{\pi(\theta)}(s)$, $i \in \mathcal{V}$ are L_i -Lipschitz continuous w.r.t. θ in \mathbb{R}^d for any $s \in \mathcal{S}$. That is, $|V_i^{\pi(\theta)}(s) - V_i^{\pi(\theta')}(s)| \leq L_i \|\theta - \theta'\|$ for any $s \in \mathcal{S}$, $\theta, \theta' \in \mathbb{R}^d$.

Assumption 2 directly implies that $J_i(\theta)$ is L_i -Lipschitz continuous. Moreover, $J(\theta)$ is L -Lipschitz continuous in \mathbb{R}^d , where $L \triangleq \sum_{i \in \mathcal{V}} L_i$, due to the following fact:

$$|J(\theta) - J(\theta')| \leq \sum_{i \in \mathcal{V}} |J_i(\theta) - J_i(\theta')| \leq \sum_{i \in \mathcal{V}} |\mathbb{E}[V_i^{\pi(\theta)}(s) - V_i^{\pi(\theta')}(s)]| \leq \sum_{i \in \mathcal{V}} L_i \|\theta - \theta'\|. \quad (11)$$

3.2 Learning Graph

Lemma 2 has shown that having the local gradient of a LVF is sufficient for each agent to update its policy according to the following gradient ascent:

$$\theta_i^{k+1} = \theta_i^k + \nabla_{\theta_i} \hat{J}_i^\delta(\theta^k), \quad i \in \mathcal{V}, \quad (12)$$

where θ^k is the policy parameter at step k , $\nabla_{\theta_i} \hat{J}_i^\delta(\theta^k)$ can be estimated by evaluating the value of $\hat{J}_i^\delta(\theta^k)$.

To ensure that each agent i has access to the value of $\hat{J}_i^\delta(\theta^k)$, in this subsection, we define the *learning graph* $\mathcal{G}_L = (\mathcal{V}, \mathcal{E}_L)$ based on the LVF design (7), which interprets the required reward information flow during the learning process. The edge set \mathcal{E}_L is defined as:

$$\mathcal{E}_L = \{(j, i) \in \mathcal{V} \times \mathcal{V} : j \in \mathcal{I}_i^L, i \in \mathcal{V}\}. \quad (13)$$

The definition of \mathcal{E}_L implies the following result.

Lemma 3 *If $(j, i) \in \mathcal{E}_L$, then $i \xrightarrow{\mathcal{E}_{COR}} j$.*

The converse of Lemma 3 is not true, see Fig. 3 as a counterexample.

To better understand the learning graph \mathcal{G}_L , we find a clustering $\mathcal{V} = \cup_{l=1}^n \mathcal{V}_l$ for the graph \mathcal{G}_{CO} , where \mathcal{V}_l is the vertex set of the l -th maximum independent strongly connected component (SCC) in

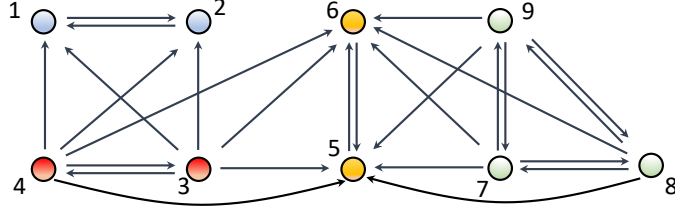


Figure 4: The learning graph \mathcal{G}_L corresponding to \mathcal{G}_{CO} in Fig. 1 and \mathcal{G}_R in Fig. 2.

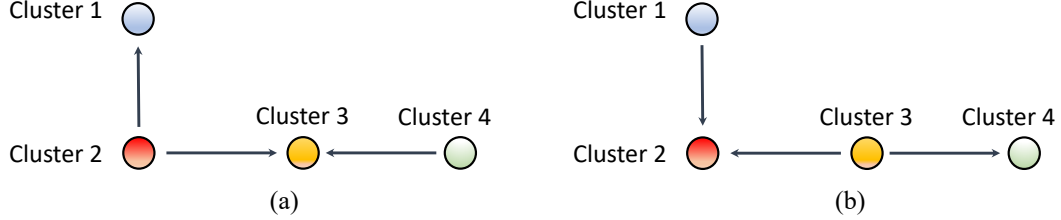


Figure 5: (a). The cluster-wise learning graph \mathcal{G}_L^{cl} . (b). The cluster-wise graph \mathcal{G}_{CO}^{cl} or \mathcal{G}_{COR}^{cl} .

\mathcal{G}_{CO} , and $\mathcal{V}_{l_1} \cap \mathcal{V}_{l_2} = \emptyset$ for any distinct $l_1, l_2 \in \mathcal{C} = \{1, \dots, n\}$. According to Lemma 1, such a clustering with $n > 1$ can always be found under Assumption 1.

According to the definition (13), we have the following observations:

- The subgraph corresponding to each cluster \mathcal{V}_i in \mathcal{G}_L is a clique.
- If there is one link in \mathcal{G}_L from one cluster to another cluster, then there is an edge in \mathcal{G}_L between any pair of agents in these two clusters.
- The agents in the same cluster share the same LVF.

To demonstrate the edge set definition (13), the learning graph corresponding to the coordination graph and the observation graph in Fig. 1, and the reward graph in Fig. 2 is shown in Fig. 4. According to the above-mentioned observations, the graph \mathcal{G}_L in Fig. 4 can be interpreted from a cluster perspective, by the graph \mathcal{G}_L^{cl} shown in Fig. 5 (a). For graphs \mathcal{G}_{CO} and \mathcal{G}_{COR} , we can also define their cluster-wise graphs \mathcal{G}_{CO}^{cl} and \mathcal{G}_{COR}^{cl} . In Example 1, due to the setting $\mathcal{G}_R = \mathcal{G}_C^\top$, it holds that $\mathcal{G}_{CO}^{cl} = \mathcal{G}_{COR}^{cl}$, as shown in Fig. 5 (b).

Note that the cluster-wise graph \mathcal{G}^{cl} for a graph \mathcal{G} is constructed by regarding each cluster as one node, and adding one edge between two clusters if there is an edge between two agents belonging to these two clusters in \mathcal{G} , respectively. However, the specific relationship between a graph and its cluster-wise version may differ, depending on the structure of the graph. More specifically, $(l_1, l_2) \in \mathcal{E}_{CO}^{cl}$ (or \mathcal{E}_{COR}^{cl}) implies that in \mathcal{G}_{CO} (or \mathcal{G}_{COR}), there exists one edge from SCC cluster \mathcal{V}_{l_1} to SCC cluster \mathcal{V}_{l_2} , in other words, any vertex in cluster \mathcal{V}_{l_2} is reachable from any vertex in cluster \mathcal{V}_{l_1} . On the other hand, $(l_1, l_2) \in \mathcal{G}_L^{cl}$ implies that there exists an edge from any vertex in cluster \mathcal{V}_{l_1} to any vertex in cluster \mathcal{V}_{l_2} . Based on these facts, we give a specific result regarding the relationship between \mathcal{G}_L^{cl} and \mathcal{G}_{CO}^{cl} as below.

Lemma 4 Given \mathcal{G}_C , \mathcal{G}_O , \mathcal{G}_R and the induced \mathcal{G}_L , the following statements are true:

- (i) $(\mathcal{E}_{CO}^{cl})^\top \subseteq \mathcal{E}_L^{cl} \subseteq (\mathcal{E}_{CO}^{cl})^\top$;
- (ii) $(\mathcal{G}_{CO}^{cl})^\top = \mathcal{G}_L^{cl} = (\mathcal{G}_{COR}^{cl})^\top$ if $\mathcal{E}_R \subseteq \mathcal{E}_{CO}^\top$;
- (iii) $(\mathcal{G}_{CO}^{cl})^\top = \mathcal{G}_L^{cl} = (\mathcal{G}_{COR}^{cl})^\top$ if and only if $i \xrightarrow{\mathcal{E}_{CO}} j$ for any $(j, i) \in \mathcal{E}_R$.

In the existing literature of MARL, it is common to see the assumption that $\mathcal{I}_i^R = \{i\}$. In this scenario, $\mathcal{E}_R = \emptyset \subseteq \mathcal{E}_{CO}$, therefore it always holds that $\mathcal{G}_L^{cl} = (\mathcal{G}_{CO}^{cl})^\top = (\mathcal{G}_{COR}^{cl})^\top$.

The learning graph \mathcal{G}_L interprets the required reward information flow in our distributed MARL algorithm. If the agents are able to exchange information via communications following \mathcal{G}_L , then each agent can acquire the information of its LVF via local communications with others. The zeroth-order oracle in [38] can then be employed to estimate $\nabla_{\theta_i} \hat{J}_i^\delta(\theta^k)$ in (12). However, \mathcal{G}_L is usually dense, inducing high communication costs, and having such a dense communication graph may be unrealistic in practice. To further relax the condition on the communication graph, in the next section, we will design a distributed RL algorithm based on local consensus algorithms.

4 Distributed RL Based on Local Consensus

In this section, we propose a distributed RL algorithm based on local consensus algorithms and ZOO with policy search in the parameter space. ZOO-based RL with policy search in the action space has been proposed in [29]. Compared to the action space, the parameter space usually has a higher dimension. However, the work in [29] requires the action space to be continuous and leverages the Jacobian of the policy π w.r.t. θ . Our RL algorithm is applicable to both continuous and discrete action spaces and even does not require π to be differentiable. In addition, our distributed learning framework based on LVFs is compatible with policy search in the action space.

4.1 Communication Weights and Distributed RL Design

We have shown that agents in the same strongly connected component share the same LVF. Therefore, there are n LVFs to be estimated. Moreover, it is unnecessary for an agent to estimate a LVF that is independent of this agent. For notation simplicity, we use \mathcal{I}_l^{cl} to denote the index set of agents involved in the LVF for the l -th cluster, $l \in \mathcal{C}$. As a result, $\mathcal{I}_l^{cl} = \mathcal{I}_i^L$ if $i \in \mathcal{V}_l$. Moreover, we denote by $n_l \triangleq |\mathcal{I}_l^{cl}|$ the number of agents involved in the LVF of cluster l .

Suppose that the communication graph $\mathcal{G}_{cm} = (\mathcal{V}, \mathcal{E}_{cm})$ is available. To make each agent obtain all the individual rewards involved in its LVF, we design a local consensus algorithm based on which the agents involved in each LVF cooperatively estimate the average of their rewards by achieving average consensus. Define n communication weight matrices $C^l \in \mathbb{R}^{N \times N}$, as follows:

$$C_{ij}^l \begin{cases} > 0, & \text{if } i, j \in \mathcal{I}_l^{cl}, (i, j) \in \mathcal{E}_{cm}; \\ = 0, & \text{otherwise,} \end{cases} \quad l \in \mathcal{C}, \quad (14)$$

where $\mathcal{C} = \{1, \dots, n\}$ is the set of indices for clusters.

We assume that given an initial state, by implementing the global policy $\pi(\theta)$, each agent is able to obtain reward $r_j^\theta(t)$, $j \in \mathcal{I}_i^L$ at each time step $t = 0, \dots, T_e - 1$. By further considering possible random effects in the transition, we rewrite the obtained local value of agent i by implementing policy $\pi(\theta)$ as $W_i(\theta, \xi) \triangleq \sum_{t=0}^{T_e-1} \gamma^t r_i^\theta(t) = \mathbb{E}[W_i(\theta, \xi)] + \xi_i$, where $\xi \in \mathbb{R}^N$ and $\xi \sim \mathcal{H}$, $\mathbb{E}[\xi_i] = 0$, $\mathbb{E}[\xi_i^2] = \sigma_i^2$, $i \in \mathcal{V}$, \mathcal{H} is determined by randomness of both the initial state and the transition probability. When a stochastic policy function is employed, \mathcal{H} is also affected by the randomness of the policy.

The distributed RL algorithm is shown in Algorithm 1. The consensus algorithm (15) is to make each agent i in cluster \mathcal{V}_l estimate $\frac{1}{n_l} \hat{W}_i(\theta^k + \delta u^k, \xi^k) = \frac{1}{n_l} \sum_{j \in \mathcal{I}_i^L} W_i(\theta^k + \delta u^k, \xi^k)$, which is the average of the reward sum among the agents involved in the corresponding LVF.

To ensure that Algorithm 1 works efficiently, we make the following assumption on graph \mathcal{G}_{cm} .

Assumption 3 *The communication graph \mathcal{G}_{cm} is undirected, and the agents specified by \mathcal{I}_l^{cl} form a connected component of \mathcal{G}_{cm} for all $l \in \mathcal{C}$.*

The following lemma gives a sufficient condition for Assumption 3.

Lemma 5 *Given that graph \mathcal{G}_{cm} is undirected, Assumption 3 holds if $\mathcal{E}_{CO} \subseteq \mathcal{E}_{cm}$.*

Algorithm 1 Distributed RL Algorithm

Input: Step-size η , initial state distribution \mathcal{D} , number of learning epochs K , number of evolution steps T_e (for policy evaluation), iteration number for consensus seeking T_c , initial policy parameter θ_0 , smoothing radius $\delta > 0$.
Output: θ^K .

1. **for** $k = 0, 1, \dots, K - 1$ **do**
2. Sample $s_0^k \sim \mathcal{D}$.
3. **for all** $i \in \mathcal{V}$ **do** (Simultaneous Implementation)
4. Agent i samples $u_i^k \sim \mathcal{N}(0, I_{d_i})$, implements policy $\pi_i(\theta_i^k + \delta u_i^k)$ for $t = 0, \dots, T_e - 1$, observes $W_i(\theta^k + \delta u^k, \xi^k)$. For $l \in \mathcal{C}$, sets $\mu_i^{kl}(0) \leftarrow W_i(\theta^k + \delta u^k, \xi^k)$ if $i \in \mathcal{I}_l^{cl}$, and sets $\mu_i^{kl}(0) \leftarrow 0$ otherwise.
5. **for** $v = 0, \dots, T_c - 1$ **do**
6. Agent i sends $\mu_i^{kl}(v)$, $l \in \mathcal{C}$ to its neighbors in \mathcal{G}_{cm} , and computes $\mu_i^{kl}(v + 1)$ according to the following updating law:

$$\mu_i^{kl}(v + 1) = \sum_{j \in \mathcal{I}_i^{cm}} C_{ij}^l \mu_j^{kl}(v). \quad (15)$$

7. **end for**
8. Agent i estimates its local gradient

$$g_i(\theta^k, u^k, \xi^k) = \frac{n_{l_i} \mu_i^{kl_i}(T_c)}{\delta} u_i^k, \quad (16)$$

where l_i denotes the cluster including i . Then agent i updates its policy according to

$$\theta_i^{k+1} = \theta_i^k + \eta g_i(\theta^k, u^k, \xi^k). \quad (17)$$

9. **end for**
10. **end for**

Proof: Note that for each cluster $l \in \mathcal{C}$, there must exist a path in \mathcal{G}_{CO} from cluster l to any agent in \mathcal{I}_l^{cl} , together with the fact that \mathcal{G}_{cm} is undirected, agents in \mathcal{I}_l^{cl} must be connected in \mathcal{G}_{cm} . \square

Once a communication graph \mathcal{G}_{cm} satisfying Assumption 3 is available, we design the communication weights such that the following assumption holds.

Assumption 4 C^l is doubly stochastic, i.e., $C^l \mathbf{1}_N = \mathbf{1}_N$ and $\mathbf{1}_N^\top C^l = \mathbf{1}_N^\top$, for all $l \in \mathcal{C}$.

Assumption 4 guarantees that average consensus can be achieved among the agents involved in each LVF. Since one agent may be involved in LVFs of multiple clusters, one agent may keep multiple different nonzero communication weights for the same communication link. From the definition of C^l in (14), $C_{jj'}^l = 0$ for all $j \notin \mathcal{I}_i^L$, and $j' \in \mathcal{V}$. Then $\mu_j^{kl}(t) = 0$ for $j \notin \mathcal{I}_i^L$ for any $p \geq 0$. Moreover, let $C_0^l \in \mathbb{R}^{n_l \times n_l}$ be the principle submatrix of C^l by removing the j -th row and column for all $j \notin \mathcal{I}_i^L$, then Assumption 4 implies that C_0^l is doubly stochastic for all $l \in \mathcal{C}$. Define $\rho_l = \|C_0^l - \frac{1}{n_l} \mathbf{1}_{n_l} \mathbf{1}_{n_l}^\top\|$, it has been shown in [39] that under Assumption 4, we have $\rho_l < 1$.

Remark 2 When graph \mathcal{G}_{CO} is strongly connected, all the agents form one cluster and achieve average consensus during the learning process. Algorithm 1 then reduces to a global consensus-based distributed RL algorithm. In fact, under any graph \mathcal{G}_{CO} , the global consensus-based framework can always solve the distributed RL problem. However, when Assumption 1 holds, our local consensus-based framework in Algorithm 1 requires consensus to be achieved among smaller-size groups, therefore exhibiting a faster convergence rate. When the whole multi-agent network is of large scale, it is possible that the number of agents involved in each LVF is significantly smaller than the number of agents in the whole network. In such scenarios, Algorithm 1 has a much faster convergence rate compared with the global consensus-based algorithm due to the following two reasons: (i) the average consensus tasks are performed within smaller-size groups; (ii) the gradient estimation based on the LVF $\hat{J}_i(\theta)$ has a lower variance compared with that based on the global value-function $J(\theta)$. See the next subsection for more details.

4.2 Convergence Analysis

In this subsection, convergence analysis of Algorithm 1 will be presented. The following assumption is made to guarantee the solvability of the problem (2).

Assumption 5 The individual reward of each agent at any time t is uniformly bounded, i.e., $r_l \leq r_i(t) \leq r_u$ for all $i \in \mathcal{V}$ and $t \in \mathbb{N}$.

Lemma 6 Under Assumption 5, there exist J_l and J_u such that $J_l \leq J_i(\theta) \leq J_u$ for any $\theta \in \mathbb{R}^d$, $i \in \mathcal{V}$.

Lemma 6 implies that there exists an optimal policy for the RL problem (4), which is the premise of solving problem (4). Based on Lemma 6, we can bound \hat{J}_i and $J = \sum_{i \in \mathcal{V}} J_i$ by $[\hat{J}_l, \hat{J}_u]$ and $[J_l, J_u]$, respectively. The following lemma bounds the error between the actual LVF and the expectation of observed LVF.

Lemma 7 Under Assumption 5, the following holds for all $l \in \mathcal{C}$ and $i \in \mathcal{V}_l$:

$$|\hat{J}_i(\theta) - \mathbb{E}[\hat{W}_i(\theta, \xi)]| \leq n_l \gamma^{T_e} J_0, \quad (18)$$

where $J_0 = \max\{|J_l|, |J_u|\} = \frac{r_0}{1-\gamma}$, $r_0 = \max\{|r_l|, |r_u|\}$, $n_l = |\mathcal{I}_i^L| = |\mathcal{I}_l^{cl}|$ is the number of agents involved in $\hat{J}_i(\theta)$.

Let $\mu^{kl} = (\dots, \mu_j^{kl}, \dots)_{j \in \mathcal{I}_i^L}^\top \in \mathbb{R}^{|\mathcal{I}_i^L|}$, the following lemma bounds the LVF estimation error.

Lemma 8 Under Assumption 1, and Assumptions 3-5. By implementing Algorithm 1, the following holds for any $l \in \mathcal{C}$ and $i \in \mathcal{V}_l$:

$$|\mathbb{E}[n_l \mu_i^{kl}(T_c)] - \hat{J}_i(\theta^k + \delta u^k)| \leq E_i, \quad (19)$$

$$\mathbb{E}_{\xi^k \sim \mathcal{H}} \left[\left[n_l \mu_i^{kl}(T_c) \right]^2 \right] \leq B_l^\mu, \quad (20)$$

where $E_i = \rho_l^{T_c} n_l^2 (J_u - J_l + \gamma^{T_e} J_0) + n_l^2 \gamma^{T_e} J_0$, $B_l^\mu = n_l^2 (\sigma_0^2 + (1 + \gamma^{T_e})^2 J_0^2)$, $\sigma_0 = \max_{i \in \mathcal{V}} \sigma_i$.

The following lemma bounds the variance of the zeroth-order oracle (16).

Lemma 9 *Under Assumptions 1, 3-5, for any $i \in \mathcal{V}_l$, it holds that $\mathbb{E}[\|g_i(\theta^k, u^k, \xi^k)\|^2] \leq \frac{B_l^\mu d_i}{\delta^2}$.*

Lemma 9 shows that the variance of each local zeroth-order oracle is mainly associated with n_l , which is the number of agents involved in the LVF for the l -th cluster. Note that if the policy evaluation is based on the global reward, the bound of $\mathbb{E}[\|g_i(\theta^k, u^k, \xi^k)\|^2]$ will be $\frac{N^2 B_l^\mu d_i}{n_l^2 \delta^2}$. When the network is of a large scale, N may be significantly larger than n_l . As a result, the variance of the zeroth-order oracle is much higher than that in our case. Therefore, our algorithm has a significantly improved scalability to large-scale networks.

Theorem 1 *Under Assumptions 1-5, let $\delta = \frac{\epsilon}{L\sqrt{d}}$, $\eta = \frac{\epsilon^{1.5}}{d^{1.5}\sqrt{K}}$. The following statements hold:*

- (i). $|J^\delta(\theta) - J(\theta)| \leq \epsilon$ for any $\theta \in \mathbb{R}^d$.
- (ii). By implementing Algorithm 1, if

$$K \geq \frac{d^3 B^2}{\epsilon^5}, \quad T_e \geq \log_\gamma \frac{\epsilon^{1.5}}{2\sqrt{2}n_0^2 L d J_0}, \quad T_c \geq \log_{\rho_0} \frac{\epsilon^{1.5}}{2\sqrt{2}n_0^2 L d (J_u - J_l + J_0)}, \quad (21)$$

then

$$\frac{1}{K} \sum_{k=0}^{K-1} \mathbb{E}[\|\nabla_\theta J^\delta(\theta^k)\|^2] \leq \epsilon, \quad (22)$$

where $B = 2(N J_u - J^\delta(\theta^0)) + L^4 n_0^2 (\sigma_0^2 + (1 + \gamma^{T_e})^2 J_0^2)$.

The convergence result provided in Theorem 1 can be alternatively written as $\frac{1}{K} \sum_{k=0}^{K-1} \mathbb{E}[\|\nabla_\theta J^\delta(\theta^k)\|^2] \leq \mathcal{O}(d^{1.5} \epsilon^{-1.5} K^{-0.5}) + \epsilon/2$. Note that the lower bounds of K , T_e and T_c are positively associated with n_0 , which is the maximal number of agents involved in one LVF. According to the definition of \mathcal{I}_i^L in (7), n_l is determined by the length of the path starting from cluster l in graph \mathcal{G}_{CO} . This implies that the convergence rate depends on the maximal length of a path in \mathcal{G}_{CO} and having shorter paths benefits for enhancing the convergence rate. When graph \mathcal{G}_{CO} is strongly connected, there is only one cluster and each path achieves its maximum length, then the distributed RL algorithm becomes a centralized algorithm based on the global value-function and the sample complexity reaches maximum. In the next section, we will provide a solution to this case.

5 Distributed RL via Truncated Local Value-Functions

Assumption 1 may not always hold in practice. According to Lemma 1, when graph \mathcal{G}_{CO} is strongly connected, $\mathcal{I}_i^L = \mathcal{V}$ for all $i \in \mathcal{V}$, namely, the LVF of each agent becomes identical to the global value-function, thereby rendering the distributed RL algorithm centralized again. Moreover, sometime even if Assumption 1 holds, the sample complexity may still be high due to the large size of some SCC or some long paths in \mathcal{G}_{CO} . In this section, motivated by [14], we resolve this issue by further dividing large size SCCs into smaller size SCCs (clusters) and ignoring agents that are far away when designing the LVF for each cluster in the graph. For each cluster, the approximation error turns out to be dependent on the distance between ignored agents and this cluster. Different from [14], where each agent neglects the effects of other agents that are far away, our design aims to make each cluster neglect its effects on other agents that are far away. Moreover, in our setting, the agents in each cluster estimate their common LVF value via local consensus, whereas in [14], each agent has its unique LVF, and it was not mentioned how this value can be obtained.

5.1 Truncated Local Value-Function Design

Different from the aforementioned SCC-based clustering for \mathcal{G}_{CO} , now we artificially give a clustering $\mathcal{V} = \cup_{l=1}^n \mathcal{V}_l$, where $\mathcal{V}_{l_1} \cap \mathcal{V}_{l_2} = \emptyset$ for distinct $l_1, l_2 \leq n$, \mathcal{V}_l still corresponds to a SCC in \mathcal{G}_{CO} . However, each cluster may no longer be a maximum SCC. That is, multiple clusters may form a larger SCC of \mathcal{G}_{CO} .

Next we define a distance function $D(i, j)$ to describe how many steps are needed for the action of agent i to affect another agent $j \in \mathcal{I}_i^L$. According to Lemma 1 (i), when $(j, i) \in \mathcal{E}_L$, there is always a path from i to j in \mathcal{G}_{COR} . Let $P(i, j)$ be the length of the shortest path ² from vertex i to vertex j in graph \mathcal{G}_{COR} . The distance function is defined as

$$D(i, j) = \begin{cases} 0, & i = j, \\ P(i, j), & (j, i) \in \mathcal{E}_L, \\ \infty, & (j, i) \notin \mathcal{E}_L. \end{cases} \quad (23)$$

We clarify the following facts regarding $D(i, j)$. (i). It may happen that there is a path from i to j in \mathcal{G}_{COR} but $(j, i) \notin \mathcal{E}_L$, see Fig. 3 as an example. Therefore, to exclude $j \notin \mathcal{I}_i^L$, we artificially defined $D(i, j)$ instead of using $P(i, j)$ directly to characterize the inter-agent distance. (ii). The distance function $D(i, j)$ defined here is unidirectional and does not satisfy the symmetry property of the distance in metric space. (iii). Although the artificial SCC clustering is obtained from \mathcal{G}_{CO} , the path length $P(i, j)$ is calculated via graph \mathcal{G}_{COR} because it always contains all the edges from i to any $j \in \mathcal{I}_i^L$. If \mathcal{G}_{CO} is used instead, some agent in \mathcal{I}_j^R , $j \in \mathcal{I}_i^L$ may be missing.

We further define the distance from a cluster l to an agent j as

$$D(\mathcal{V}_l, j) = \min_{i \in \mathcal{V}_l} D(i, j). \quad (24)$$

Denote by $D_l^* = \max_{j \in \mathcal{V}} D(\mathcal{V}_l, j)$ the maximum distance from cluster l to any agent out of this cluster that can be affected by cluster l . Since we have defined $n_l = |\mathcal{I}_l^L|$, it is observed that $D_l^* = n_l - |\mathcal{V}_l|$.

Given a cluster $l \in \mathcal{C}$, for any agent $i \in \mathcal{V}_l$, we define the following TLVF:

$$\tilde{J}_i^\delta(\theta) = \begin{cases} \sum_{j \in \mathcal{I}_i^L} J_j^\delta(\theta), & \kappa \geq D_l^*, \\ \sum_{j \in \mathcal{V}_l^\kappa} J_j^\delta(\theta), & \kappa < D_l^*, \end{cases} \quad (25)$$

where $\mathcal{V}_l^\kappa = \{j \in \mathcal{V} : D(\mathcal{V}_l, j) \leq \kappa\}$ is the set of agents involved in the TLVF of cluster l , $\kappa \in \mathbb{N}_+$ is a pre-specified truncation index determining the maximum number of agents other than cluster l that are involved in the LVF of cluster l .

The following lemma bounds the error between the local gradients of the TLVF and the global value function.

Lemma 10 *Under Assumption 2. Given cluster l , and agent $i \in \mathcal{V}_l$, the following bound holds for $\tilde{J}_i^\delta(\theta)$:*

$$\|\nabla_{\theta_i} \tilde{J}_i^\delta(\theta) - \nabla_{\theta_i} J^\delta(\theta)\| \leq \gamma^{\kappa+1} \sum_{j \in \bar{\mathcal{V}}_l^\kappa} L_j \sqrt{dd_i}, \quad (26)$$

where $\bar{\mathcal{V}}_l^\kappa = \{j \in \mathcal{V} : \kappa < D(\mathcal{V}_l, j) < \infty\} = \mathcal{V}_l \setminus \mathcal{V}_l^\kappa$.

Lemma 10 implies that the error between $\nabla_{\theta_i} \tilde{J}_i^\delta(\theta)$ and $\nabla_{\theta_i} J^\delta(\theta)$ exponentially decays with the exponent κ . Therefore, when $\gamma^{\kappa+1}$ is sufficiently small, by employing $\nabla_{\theta_i} \tilde{J}_i^\delta(\theta)$ in the gradient ascent algorithm, the induced error should be acceptable. This is the fundamental idea of our approach. In next subsection, we will propose the detailed algorithm design and convergence analysis.

²The length of a path refers to the number of edges included in this path.

5.2 Distributed RL with Convergence Analysis

Next we design a distributed RL algorithm based on the TLVF. It suffices to redesign the communication weights, so that the value of $\tilde{J}_i^\delta(\theta)$ (instead of $\hat{J}_i^\delta(\theta)$) can be estimated for each agent $i \in \mathcal{V}$. For any cluster $l \in \mathcal{C}$, instead of using \mathcal{I}_l^{cl} , we set the index set of agents involved in the LVF as $\mathcal{I}_l^\kappa = \mathcal{I}_l^{cl} \cap \mathcal{V}_l^\kappa$.

Define the number of agents involved in each TLVF as

$$n_l^\kappa = \begin{cases} n_l, & \kappa \geq D_l^*, \\ |\mathcal{V}_l| + \kappa, & \kappa < D_l^*. \end{cases} \quad (27)$$

Recall that $D_l^* = n_l - |\mathcal{V}_l|$, it always holds that $n_l^\kappa \leq n_l$.

The l -th communication weight matrix is then redesigned as

$$C_{ij}^{l,\kappa} = \begin{cases} > 0, & \text{if } i, j \in \mathcal{I}_l^\kappa, (i, j) \in \mathcal{E}_{cm}; \\ = 0, & \text{otherwise,} \end{cases} \quad l \in \mathcal{C}, \quad (28)$$

where $\mathcal{C} = \{1, \dots, n\}$.

Similar to Assumptions 3 and 4, we make the following two assumptions.

Assumption 6 *The communication graph \mathcal{G}_{cm} is undirected, and and the agents specified by \mathcal{I}_l^κ form a connected component of \mathcal{G}_{cm} for all $l \in \mathcal{C}$.*

Assumption 7 *$C^{l,\kappa}$ is doubly stochastic for all $l \in \mathcal{C}$.*

Note that Assumption 6 is milder than Assumption 3 because $\mathcal{I}_l^\kappa \subseteq \mathcal{I}_l^{cl}$, implying that fewer communication links are needed when the TLVF method is employed. Moreover, when the communication graph \mathcal{G}_{cm} is available, κ can be designed to meet Assumption 7.

The distributed RL algorithm based on TLVFs can be obtained by simply replacing the communication weight matrices C^l with $C^{l,\kappa}$, for all $l \in \mathcal{C}$.

Similar to Lemmas 7, 8 and 9, we have the following results.

Lemma 11 *Under Assumption 5, the following holds for all $l \in \mathcal{C}$ and $i \in \mathcal{V}_l$:*

$$|\tilde{J}_i(\theta) - \mathbb{E}[\tilde{W}_i(\theta, \xi)]| \leq n_l^\kappa \gamma^{T_e} J_0. \quad (29)$$

Lemma 12 *Under Assumption 1, Assumptions 5-7. By implementing Algorithm 1, the following holds for any $l \in \mathcal{C}$ and $i \in \mathcal{V}_l$:*

$$|\mathbb{E}[n_l \mu_i^{kl}(T_c)] - \tilde{J}_i(\theta^k + \delta u^k)| \leq E_i^\kappa, \quad (30)$$

$$\mathbb{E}_{\xi^k \sim \mathcal{H}} \left[[n_l \mu_i^{kl}(T_c)]^2 \right] \leq B_l^\kappa, \quad (31)$$

where $E_i^\kappa = (\rho_l^\kappa)^{T_c} (n_l^\kappa)^2 (J_u - J_l + \gamma^{T_e} J_0) + (n_l^\kappa)^2 \gamma^{T_e} J_0$, $B_l^\kappa = (n_l^\kappa)^2 (\sigma_0^2 + (1 + \gamma^{T_e})^2 J_0^2)$, $\sigma_0 = \max_{i \in \mathcal{V}} \sigma_i$, $\rho_l^\kappa = \|C_0^{l,\kappa} - \frac{1}{n_l^\kappa} \mathbf{1}_{n_l^\kappa} \mathbf{1}_{n_l^\kappa}^\top\|$.

Lemma 13 *Under Assumptions 1, 5-7, for any $i \in \mathcal{V}_l$, it holds that $\mathbb{E}[\|g_i(\theta^k, u^k, \xi^k)\|^2] \leq \frac{B_l^\kappa d_i}{\delta^2}$.*

Theorem 2 *Under Assumptions 1, 2, 5-7, let $\delta = \frac{\epsilon}{L\sqrt{d}}$, $\eta = \frac{\epsilon^{1.5}}{d^{1.5}\sqrt{K}}$. The following statements hold:*

- (i). $|J^\delta(\theta) - J(\theta)| \leq \epsilon$ for any $\theta \in \mathbb{R}^d$.
- (ii). By implementing Algorithm 1, if

$$K \geq \frac{d^3 B^2}{\epsilon^5}, \quad T_e \geq \log_\gamma \frac{\epsilon^{1.5}}{4(n_0^\kappa)^2 L d J_0}, \quad T_c \geq \log_{\rho_0} \frac{\epsilon^{1.5}}{4(n_0^\kappa)^2 L d (J_u - J_l + J_0)}, \quad (32)$$

then

$$\frac{1}{K} \sum_{k=0}^{K-1} \mathbb{E}[\|\nabla_\theta J^\delta(\theta^k)\|^2] \leq \epsilon + \gamma^{\kappa+1} \max_{l \in \mathcal{C}} |\bar{\mathcal{V}}_l^\kappa| L_0 \sqrt{d d_0}, \quad (33)$$

where $B = 2(N J_u - J^\delta(\theta^0)) + (n_0^\kappa)^2 (\sigma_0^2 + (1 + \gamma^{T_e})^2 J_0^2) L^4$, $n_0^\kappa = \max_{l \in \mathcal{C}} n_l^\kappa$.

Remark 3 The sample complexity provided in Theorem 2 is associated with n_0^κ , which may be significantly smaller than n_0 (depending on κ) in Theorem 1. On the other hand, the convergence error in Theorem 2 has an extra term associated with $\gamma^{\kappa+1}$. Therefore, there is a trade off when we choose κ . The greater κ is, the smaller the convergence error will be, however, the convergence rate may be decreased. For example, when $\gamma = 0.6$, we have $\gamma^{\kappa+1} \leq 0.028$ if $\kappa \geq 6$. In this case, we can choose $\kappa = 6$, implying that each cluster only consider its effects on 6 agents other than this cluster even when \mathcal{G}_{CO} is strongly connected. Therefore, when the network is of a huge scale with long paths in graph \mathcal{G}_{CO} , using the TLVFs can further reduce the sample complexity.

6 Discussions on Distributed RL with Two-Point Feedback

The two distributed RL algorithms proposed in the last two sections are based on the one-point zeroth-order oracle (16). We observe that Algorithm 1 is always efficient as long as $g(\theta^k, u^k, \xi^k)$ is an unbiased estimate of $\nabla_\theta J^\delta(\theta^k)$ and $\mathbb{E}[\|g(\theta^k, u^k, \xi^k)\|^2]$ is bounded. Therefore, the two-point feedback oracles proposed in [38] and the residual feedback oracle in [40] can also be employed in Algorithm 1. Based on the LVF design in our work, the two-point feedback oracle for each agent i at learning episode k can be obtained as

$$\bar{g}_i(\theta^k, u^k, \xi^k) = \frac{\mu_i^{kl_i}(T_c) - \nu_i^{kl_i}(T_c)}{\delta} n_{l_i} u_i^k, \quad (34)$$

where $\nu_i^{kl_i}(T_c)$ is the approximate estimation of $\hat{W}_i(\theta^k, \zeta^k)/n_{l_i}$ via local consensus.

Define $\hat{L}_i = \sum_{j \in \mathcal{I}_i^L} L_i$, which is a Lipschitz constant of \hat{W}_i . Then we can show

$$\begin{aligned} \mathbb{E}[\|\bar{g}_i(\theta^k, u^k, \xi^k)\|^2] &= \mathbb{E}[\|\frac{\hat{J}_i(\theta^k + \delta u^k) - \hat{J}_i(\theta^k) + n_{l_i} \mu_i^{kl_i}(T_c) - \hat{J}_i(\theta^k + \delta u^k) + \hat{J}_i(\theta^k) - n_{l_i} \nu_i^{kl_i}(T_c)}{\delta} u_i^k\|^2] \\ &= \mathbb{E}[\|\frac{\hat{J}_i(\theta^k + \delta u^k) - \hat{J}_i(\theta^k) + \mathbb{E}[n_{l_i} \mu_i^{kl_i}(T_c)] - \hat{J}_i(\theta^k + \delta u^k) + \hat{J}_i(\theta^k) - \mathbb{E}[n_{l_i} \nu_i^{kl_i}(T_c)] + \sum_{j \in \mathcal{I}_i^L} (\xi_j^k - \zeta_j^k)}{\delta} u_i^k\|^2] \\ &\leq 2\mathbb{E}[\hat{L}_i^2 \|u^k\|^2 \|u_i^k\|^2] + 2((2E_i)^2 + 2n_l \sigma_0^2) \mathbb{E}[\|u_i^k\|^2/\delta^2] \\ &\leq 2\hat{L}_i^2 \left(\mathbb{E}[\|u_i\|^4] + \mathbb{E}[\sum_{j \in \mathcal{V} \setminus \{i\}} \|u_j\|^2] \mathbb{E}[\|u_i\|^2] \right) + 4(2E_i^2 + n_l \sigma_0^2) d_i/\delta^2 \\ &\leq 2\hat{L}_i^2 ((d_i + 4)^2 + (d - d_i)d_i) + 4(2E_i^2 + n_l \sigma_0^2) d_i/\delta^2 \\ &= 2\hat{L}_i^2 (d_i d + 8d_i + 16) + 4(2E_i^2 + n_l \sigma_0^2) d_i/\delta^2, \end{aligned} \quad (35)$$

where $\xi = (\xi_1, \dots, \xi_N)^\top$ and $\zeta = (\zeta_1, \dots, \zeta_N)^\top$ are the noises in the observations $W_i(\theta^k + \delta u^k, \xi^k)$ and $W_i(\theta^k, \zeta^k)$, respectively, i.e., $W_i(\theta^k + \delta u^k, \xi^k) = \mathbb{E}[W_i(\theta^k + \delta u^k, \xi^k)] + \xi_i$, $W_i(\theta^k, \zeta^k) = \mathbb{E}[W_i(\theta^k, \zeta^k)] + \zeta_i$; the first inequality used the bound E_i in (19) and the assumptions $\mathbb{E}[\xi_i] = \mathbb{E}[\zeta_i] = 0$ and $\mathbb{E}[\xi_i^2] \leq \sigma_0$, $i \in \mathcal{V}$.

Comparisons with one-point feedback. Note that E_i can be arbitrarily small as long as T_e and T_c are sufficiently large. Let us first consider the ideal case where the consensus estimation is perfect $T_c = \infty$ and the observation is exact, i.e., $W_i = \mathbb{E}[W_i] = J_i$ ($T_e = \infty$ and $\xi = 0$), then $E_i = 0$ and $\sigma_0 = 0$. As a result, the upper bound of $\mathbb{E}[\|\bar{g}_i(\theta^k, u^k, \xi^k)\|^2]$ is independent of δ , whereas the upper bound of $\mathbb{E}[\|g_i(\theta^k, u^k, \xi^k)\|^2]$ becomes $n_l^2 J_0^2 d_i/\delta^2$, as shown in Lemma 9. This implies that the variance of the two-point zeroth-order oracle is independent of the reward value and the maximum path length n_0 , thus is more scalable than the one-point feedback. Now we consider a more practical scenario where both the consensus estimations and the observations are inexact. For convenience of analysis, we consider $\delta > 0$ as an infinitesimal quantity and neglect terms in the upper bounds independent of the network scale. Then we have $\mathbb{E}[\|\bar{g}_i(\theta^k, u^k, \xi^k)\|^2] = \mathcal{O}(n_l d_i/\delta^2)$. In Lemma 9, we showed that the variance bound for the zeroth-order oracle with one-point feedback is $\mathcal{O}(n_l^2 d_i/\delta^2)$. Therefore, when $\delta > 0$ is small enough, the two-point zeroth-order oracle still outperforms the one-point feedback scheme in terms of lower variance and faster convergence speed.

7 Simulation Results

In this section, we present two examples, where the first one shows the results of applying Algorithm 1 with the communication weight matrices (14) to the resource allocation problem in Example 1, and the second one shows the results of applying Algorithm 1 with the communication weight matrices (28) to a large-scale network scenario.

Example 2 We employ the distributed RL with LVFs in (9) to solve the problem in Example 1. To seek the optimal policy $\pi_i(o_i)$ for agent i to determine its action $\{a_{ij}\}_{j \in \mathcal{N}_i}$, we parameterize the policy function by defining

$$a_{ij} = \frac{\exp(-z_{ij})}{\sum_{j \in \mathcal{I}_i} \exp(-z_{ij})}, \quad (36)$$

where z_{ij} is approximated by radial basis functions:

$$z_{ij} = \sum_{k=1}^{n_c} \|o_i - c_{ik}\|^2 \theta_{ij}(k), \quad (37)$$

$c_{ik} = (\hat{c}_{ik}^\top, \bar{c}_{ik}) \in \mathbb{R}^{|\mathcal{I}_i|+1}$ is the center of the k -th feature for agent i , here $\hat{c}_{ik} \in \mathbb{R}^{|\mathcal{I}_i|}$ and \bar{c}_{ik} are set according to the ranges of $m_{\mathcal{I}_i}$ and d_i , respectively, such that c_{ik} , $k = 1, \dots, n_c$ are approximately evenly distributed in the range of o_i .

Set $m_i(0) = 1 + \chi_i$ for all $i = 1, \dots, 9$, χ_i is a random variable with zero mean and is bounded by 0.01, the number of evolution steps $T_e = 10$, and the number of learning epochs $K = 600$, $y_i(t) - d_i(t) = 0.5 \sin t$. The communication graph $\mathcal{G}_{cm} = (\mathcal{V}, \mathcal{E}_{cm})$ is set as $\mathcal{G}_{cm} = \mathcal{G}_{CO} \cup \mathcal{G}_{CO}^\top$, which satisfies Assumption 3. Let G_{cm} be the 0-1 weighted matrix of graph \mathcal{G}_{cm} , that is, $G_{cm}(i, j) = 1$ if $(i, j) \in \mathcal{E}_{cm}$ and $G_{cm}(i, j) = 0$ otherwise. Let $d_i^{cm} = \sum_{(j,i) \in \mathcal{E}_{cm}} G_{cm}(i, j)$. The communication weights are set as Metropolis weights [41]:

$$C_{ij}^l = \begin{cases} \frac{1}{1 + \max\{d_i^{cm}, d_j^{cm}\}}, & \text{if } i \neq j, i, j \in \mathcal{I}_l^{cl}, (i, j) \in \mathcal{E}_{cm}; \\ 1 - \sum_{j \neq i} C_{ij}^l, & \text{if } i = j; \\ 0, & \text{otherwise,} \end{cases} \quad l \in \mathcal{C}. \quad (38)$$

By further setting the consensus iteration number $T_c = 10$, $\eta = 0.01$, and $\delta = 2$, Fig. 6 (left) depicts the evolution of the observed values of the global value-function by implementing 4 different algorithms repeatedly for 10 times. Here ξ^* denotes the noise generated in the simulation. In each time of implementation, one perturbation vector u^k is sampled and used for all the 4 algorithms during each learning episode k . The centralized algorithm is the zeroth-order optimization algorithm based on global value evaluation, while the distributed algorithm is based on local value evaluation (Algorithm 1). The distributed two-point feedback algorithm is Algorithm 1 with $g_i(\theta^k, u^k, \xi^k)$ replaced by $\bar{g}_i(\theta^k, u^k, \xi^k)$ in (34). We observe that the distributed algorithms are always faster than the centralized algorithms. Fig. 6 (middle) and Fig. 6 (right) show the comparison of centralized and distributed one-point feedback algorithms, and the comparison of centralized and distributed two-point feedback algorithms, respectively. From these two figures, it is clear that the distributed algorithms always exhibit lower variances in contrast to the centralized algorithms. This implies that the policy evaluation based on LVFs is more robust than policy evaluation based on the global value-function.

Example 3 Next, in a setting similar to Example 1, we consider a large-size case where there are 100 warehouses. The coordination graph \mathcal{G}_C and the observation graph have the same edge set:

$$\mathcal{E}_C = \mathcal{E}_O = \{(i, j) \in \mathcal{V}^2 : |i - j| = 1, i = 2k - 1, k \in \mathbb{N}\} \cup \{(1, N)\}.$$

The reward graph is set as $\mathcal{G}_R = \mathcal{G}_C^\top$. Accordingly, graph $\mathcal{G}_L = (\mathcal{V}, \mathcal{E}_L)$ has the edge set

$$\mathcal{E}_L = \{(i, j) \in \mathcal{V}^2 : |i - j| = 1, i = 2k, k \in \mathbb{N}\} \cup \{(N, 1)\}.$$

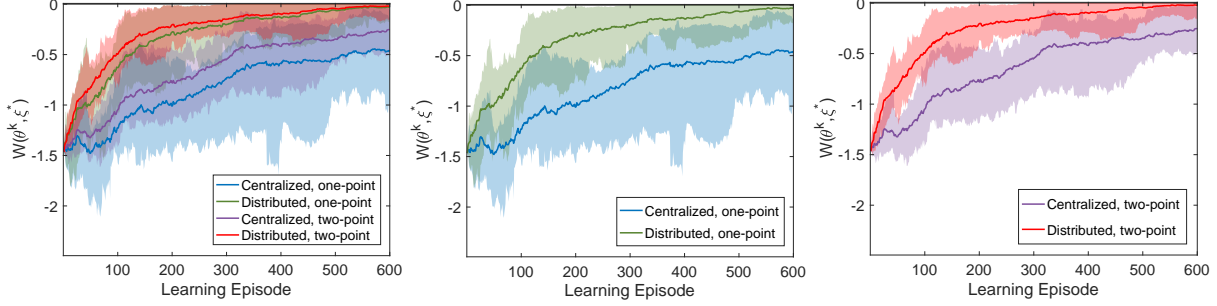


Figure 6: **(Left)** Comparison of different algorithms for 9 warehouses; **(Middle)** centralized and distributed algorithms under zeroth-order oracles with one-point feedback; **(Right)** centralized and distributed algorithms under zeroth-order oracles with two-point feedback.

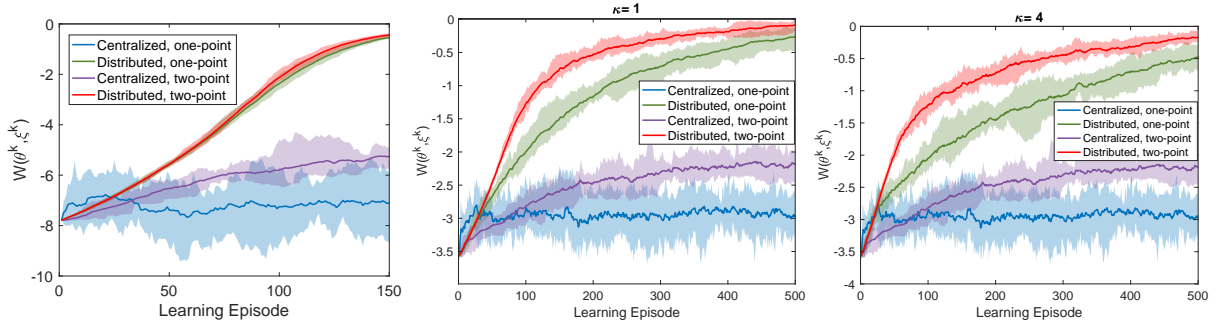


Figure 7: **(Left)** Comparison of different algorithms for Example 3; **(Middle)** comparison of different algorithms for Example 4 with $\kappa = 1$; **(Right)** comparison of different algorithms for Example 4 with $\kappa = 4$.

The communication graph $\mathcal{G}_{cm} = (\mathcal{V}, \mathcal{E}_{cm})$ is still set as $\mathcal{G}_{cm} = \mathcal{G}_{CO} \cup \mathcal{G}_{CO}^\top$. Other parameter settings are the same as those in Example 2. Fig. 7 (left) shows the evolutions of the observed values of the global value-function by implementing 4 different algorithms repeatedly for 10 times. Observe that when the network is of a large scale, policy evaluation based on the global value-function becomes very unstable due to the high variance of the gradient estimates. On the contrary, our distributed algorithms based on observing LVFs are more robust and exhibit significantly lower variances. Moreover, the two-point oracle always outperforms the one-point oracle in terms of lower variance and faster convergence. These observations are consistent with our analysis in Remark 2 and Section 6.

Example 4 Now we consider 100 warehouses with a connected undirected coordination graph. The coordination graph \mathcal{G}_C and the observation graph have the same edge set:

$$\mathcal{E}_C = \mathcal{E}_O = \{(i, j) \in \mathcal{V}^2 : |i - j| = 1\} \cup \{(1, N), (N, 1)\}.$$

The edge set of graph $\mathcal{G}_R = (\mathcal{V}, \mathcal{E}_R)$ is set as $\mathcal{E}_R = \emptyset$, implying that the individual reward of each agent only depends on its own state and action. In this case, the learning graph \mathcal{G}_L is complete because $i \xrightarrow{\mathcal{E}_{CO}} j$ for any $i, j \in \mathcal{V}$. Then Algorithm 1 with the LVF setting in (9) becomes a centralized algorithm. Hence, we employ the TLVF defined in (25). The communication graph is set as $\mathcal{G}_{cm} = \mathcal{G}_C$. By choosing same parameters $m_i(0)$, T_e , T_c , $y_i(t) - d_i(t)$ as those in Example 2, as generating matrices C_{ij}^l in the same way as that in (38), the simulation results with $\kappa = 1$ and $\kappa = 4$ are shown in Fig. 7 (Middle) and Fig. 7 (Right), respectively. From the simulations, we observe that our distributed RL algorithm with

$\kappa = 1$ and two-point feedback has the lowest variance and fastest convergence rate, which is consistent with our analysis in Remark 3. Moreover, the approximation error induced by $\kappa = 1$ does not affect the significantly improved performance of our RL algorithm compared with GVF-based centralized algorithms.

8 Conclusions

We have recognized three graphs inherently embedded in MARL, namely, coordination graph, observation graph, and reward graph. A connection between these three graphs and the learning graph was established, based on which we proposed our distributed RL algorithm via LVFs and derived conditions on the communication graph required in RL. It was shown that the LVFs constructed based on the aforementioned 3 graphs are able to play the same role as the GVF in gradient estimation. To adapt our algorithm to MARL with general graphs, we have designed TLVFs associated with an artificially specified index. The choice of this index is a trade off between variance reduction and gradient approximation errors. Simulation examples have shown that our proposed algorithms with LVFs or TLVFs significantly outperform RL algorithms based on GVF, especially for large-scale MARL problems.

The RL algorithms proposed in this work are policy gradient algorithms based on ZOO, which are general, but may be not the best choice for specific applications. In the future, we are interested in exploring how our distributed graph-theoretic approach can be combined with other RL techniques to facilitate learning for large-scale network systems.

9 Appendix: Proofs of Lemmas and Theorems

Proof of Lemma 2: Define

$$\bar{J}_i(\theta) = J(\theta) - \hat{J}_i(\theta) = \sum_{j \in \mathcal{V} \setminus \mathcal{I}_i^L} \mathbb{E}_{s_0 \sim \mathcal{D}} V_j^{\pi(\theta)}(s_0). \quad (39)$$

Next we show that $\bar{J}_i(\theta)$ is independent of θ_i .

Let \mathcal{N}_i^{CO-} be the set of vertices in graph \mathcal{G}_{CO} that can reach i and $\mathcal{I}_i^{CO-} = \mathcal{N}_i^{CO-} \cup \{i\}$. Note that for each agent j , its action at time t , i.e., $a_j(t)$, is only affected by the partial observation $o_j(t)$, the current state $s_j(t)$, and policy θ_j . Therefore, there exists a function $f_j : \mathcal{O}_j \times \mathbb{R}^{d_j} \rightarrow P(\mathcal{A}_j)$ such that

$$a_j(t) \sim f_j(o_j(t), \theta_j) = f_j(\{s_k(t)\}_{k \in \mathcal{I}_j^O}, \theta_j). \quad (40)$$

Similarly, according to the definition of \mathcal{P}_i , there exists another function $h_j : \Pi_{k \in \mathcal{I}_j^C} \mathcal{S}_k \times \Pi_{k \in \mathcal{I}_j^C} \mathcal{A}_k \rightarrow P(\mathcal{S}_j)$ such that

$$s_j(t) \sim h_j(\{s_k(t-1)\}_{k \in \mathcal{I}_j^C}, \{a_k(t-1)\}_{k \in \mathcal{I}_j^C}), \quad (41)$$

together with (40), we have

$$s_j(t) \sim h_j(\{s_k(t-1)\}_{k \in \mathcal{I}_j^{CO}}, \{\theta_l\}_{l \in \mathcal{I}_j^C}), \quad (42)$$

and

$$a_j(t) \sim f_j(\{h_k(\{s_{l1}(t-1)\}_{l1 \in \mathcal{I}_k^{CO}}, \{\theta_{l2}\}_{l2 \in \mathcal{I}_k^C})\}_{k \in \mathcal{I}_j^O}, \theta_j), \quad (43)$$

where $\mathcal{I}_j^{CO} = \mathcal{I}_j^C \cup \mathcal{I}_j^O$.

According to (42) and (43), we conclude that $\{s_j(t), a_j(t)\}$ is affected by θ_l only if $l \in \mathcal{I}_j^{CO-}$. As a result, $\{s_k(t), a_k(t)\}_{k \in \mathcal{I}_j^R}$ is affected by θ_l only if $l \in \bigcup_{k \in \mathcal{I}_j^R} \mathcal{I}_k^{CO-} \triangleq A_j$.

Next we show once $j \notin \mathcal{I}_i^L$, it must hold that $i \notin A_j$. By the definition in (7), $j \notin \mathcal{I}_i^L$ implies that $\mathcal{I}_j^R \cap \mathcal{I}_i^{CO+} = \emptyset$. That is, there are no vertices in \mathcal{I}_j^R that are reachable from vertex i in graph \mathcal{G}_{CO} . As a result, $i \notin A_j$.

Then we conclude that θ_i never influences $r_j(s_{\mathcal{I}_i^R}(t), a_{\mathcal{I}_i^R}(t))$ for any $t \geq 0$ if $j \notin \mathcal{I}_i^L$. Therefore, $\bar{J}_i(\theta)$ is independent of θ_i .

Proof for (i): it has been shown in [38] that

$$\nabla_\theta J^\delta(\theta) = \frac{1}{\delta\varphi} \int_{\mathbb{R}^d} J(\theta + \delta u) e^{-\frac{1}{2}\|u\|^2} u du, \quad (44)$$

where

$$\varphi = \int_{\mathbb{R}^d} e^{-\frac{1}{2}\|u\|^2} du. \quad (45)$$

Define

$$\Phi^i = (\mathbf{0}_{d_i \times d_1}, \dots, I_{d_i}, \dots, \mathbf{0}_{d_i \times d_N}) \in \mathbb{R}^{d_i \times d}, \quad (46)$$

then $u_i = \Phi^i u$. It follows that

$$\begin{aligned} \nabla_{\theta_i} J^\delta(\theta) &= \Phi^i \nabla_\theta J^\delta(\theta) \\ &= \frac{1}{\delta\varphi} \int_{\mathbb{R}^d} J(\theta + \delta u) e^{-\frac{1}{2}\|u\|^2} u_i du \\ &= \frac{1}{\delta\varphi} \int_{\mathbb{R}^d} \hat{J}_i(\theta + \delta u) e^{-\frac{1}{2}\|u\|^2} u_i du \\ &\quad + \frac{1}{\delta\varphi} \int_{\mathbb{R}^d} \bar{J}_i(\theta + \delta u) e^{-\frac{1}{2}\|u\|^2} u_i du. \end{aligned} \quad (47)$$

Let $\bar{\theta}_i = (\dots, \theta_j^\top, \dots)_{j \neq i}^\top \in \mathbb{R}^{d-d_i}$, $\bar{u}_i = (\dots, u_j^\top, \dots)_{j \neq i}^\top \in \mathbb{R}^{d-d_i}$. Since we have proved that $\bar{J}_i(\theta + \delta u)$ is independent of u_i , the following holds:

$$\begin{aligned} &\int_{\mathbb{R}^d} \bar{J}_i(\theta + \delta u) e^{-\frac{1}{2}\|u\|^2} u_i du \\ &= \int_{\mathbb{R}^{d-d_i}} \bar{J}_i(\bar{\theta}_i + \delta \bar{u}_i) e^{-\frac{1}{2}\|\bar{u}_i\|^2} d\bar{u}_i \int_{\mathbb{R}^{d_i}} e^{-\frac{1}{2}\|u_i\|^2} u_i du_i \\ &= 0. \end{aligned}$$

Therefore,

$$\nabla_{\theta_i} J^\delta(\theta) = \frac{1}{\delta\varphi} \int_{\mathbb{R}^d} \hat{J}_i(\theta + \delta u) e^{-\frac{1}{2}\|u\|^2} u_i du = \nabla_{\theta_i} \hat{J}_i^\delta(\theta). \quad (48)$$

Proof for (ii): differentiability of $J_i(\theta)$ for all $i \in \mathcal{V}$ implies that $\hat{J}_i(\theta)$ for all $i \in \mathcal{V}$ and $J(\theta)$ are differentiable as well. Since $\bar{J}_i(\theta)$ is independent of θ_i , we have

$$\nabla_{\theta_i} J(\theta) = \nabla_{\theta_i} (\hat{J}_i(\theta) + \bar{J}_i(\theta)) = \nabla_{\theta_i} \hat{J}_i(\theta). \quad (49)$$

This completes the proof. \square

Proof of Lemma 4: (i). Given $(l_1, l_2) \in \mathcal{E}_{CO}^{cl}$, there must hold that $i \xrightarrow{\mathcal{E}_{CO}} j$ for any $i \in \mathcal{V}_{l_1}$ and $j \in \mathcal{V}_{l_2}$. Due to the definition of \mathcal{G}_L , $(j, i) \in \mathcal{E}_L$ for any $i \in \mathcal{V}_{l_1}$ and $j \in \mathcal{V}_{l_2}$, implying that $(l_1, l_2) \in (\mathcal{E}_L^{cl})^\top$. Therefore, $\mathcal{E}_{CO}^{cl} \subseteq (\mathcal{E}_L^{cl})^\top$. It follows that $(\mathcal{E}_{CO}^{cl})^\top \subseteq \mathcal{E}_L^{cl}$.

On the other hand, for any $(l_1, l_2) \in \mathcal{E}_L^{cl}$, we have $(i, j) \in \mathcal{E}_L$ for any $i \in \mathcal{V}_{l_1}$ and $j \in \mathcal{V}_{l_2}$. According to Lemma 3, $j \xrightarrow{\mathcal{E}_{CO}^{cl}} i$ for any $i \in \mathcal{V}_{l_1}$ and $j \in \mathcal{V}_{l_2}$. Hence, $(l_1, l_2) \in (\mathcal{E}_{CO}^{cl})^\top$.

(ii). By the virtue of statement (i), it suffices to show that $\mathcal{G}_{CO}^{cl} = \mathcal{G}_{COR}^{cl}$ if $\mathcal{E}_R \subseteq \mathcal{E}_{CO}^\top$, which is true due to the definition of \mathcal{G}_{COR} .

(iii). Note that $\mathcal{G}_{CO}^{cl} = \mathcal{G}_{COR}^{cl}$ is equivalent to the statement that there is a path from i to j in \mathcal{G}_{CO} if and only if there is a path from i to j in \mathcal{G}_{COR} , which is equivalent to the statement that adding the edges of \mathcal{E}_R^\top to \mathcal{G}_{CO} does not change the reachability between any two nodes in \mathcal{G}_{CO} . This holds if and only if j is reachable from i for any $(i, j) \in \mathcal{E}_R$. \square

Proof of Lemma 6: Given any policy $\pi(\theta)$, it holds that

$$\sum_{t=0}^{\infty} \gamma^t r_i(s_i(t), a_i(t)) \leq \sum_{t=0}^{\infty} \gamma^t r_u = \frac{1}{1-\gamma} r_u \triangleq J_u. \quad (50)$$

Similarly, it can be shown that $J_l = \frac{1}{1-\gamma} r_l$. \square

Proof of Lemma 7: From the definition of $J_i(\theta)$ and $W_i(\theta, \xi)$, we have

$$|J_i(\theta) - \mathbb{E}[W_i(\theta, \xi)]| = \left| \mathbb{E} \left[\sum_{t=T_e}^{\infty} \gamma^t r_i(s_i(t), a_i(t)) \right] \right| \leq \sum_{t=T_e}^{\infty} \gamma^t r_0 = \frac{\gamma^{T_e}}{1-\gamma} r_0. \quad (51)$$

Then we have

$$|\hat{J}_i(\theta) - \mathbb{E}[\hat{W}_i(\theta, \xi)]| \leq \sum_{j \in \mathcal{I}_i^L} |J_j(\theta) - \mathbb{E}[W_j(\theta, \xi)]| \leq \frac{n_l \gamma^{T_e}}{1-\gamma} r_0. \quad (52)$$

The proof is completed. \square

Proof of Lemma 8: Note that the following holds for any step v :

$$\sum_{j \in \mathcal{I}_i^L} \mu_j^{kl}(v+1) = \mathbf{1}_{n_l}^\top \mu^{kl}(v+1) = \mathbf{1}_{n_l}^\top C_0^l \mu^{kl}(v) = \mathbf{1}_{n_l}^\top \mu^{kl}(v), \quad (53)$$

where the last equality holds because C_0^l is doubly stochastic. It follows that $\mathbf{1}_{n_l}^\top \mu^{kl}(v) = \hat{W}_i(\theta^k + \delta u^k, \xi^k)$ for any $v \in [0, T_c]$.

Next we evaluate the estimation error. The following holds:

$$\begin{aligned} n_l \mu^{kl}(v) - \mathbf{1}_{n_l} \hat{W}_i(\theta^k + \delta u^k, \xi^k) &= n_l \mu^{kl}(v) - \mathbf{1}_{n_l} \mathbf{1}_{n_l}^\top \mu^{kl}(v) \\ &= n_l C_0^l \mu^{kl}(v-1) - \mathbf{1}_{n_l} \mathbf{1}_{n_l}^\top \mu^{kl}(v-1) \\ &= (C_0^l - \frac{1}{n_l} \mathbf{1}_{n_l} \mathbf{1}_{n_l}^\top)(n_l \mu^{kl}(v-1) - \mathbf{1}_{n_l} \mathbf{1}_{n_l}^\top \mu^{kl}(v-1)) \\ &= (C_0^l - \frac{1}{n_l} \mathbf{1}_{n_l} \mathbf{1}_{n_l}^\top)^v (n_l \mu^{kl}(0) - \mathbf{1}_{n_l} \mathbf{1}_{n_l}^\top \mu^{kl}(0)) \\ &= (C_0^l - \frac{1}{n_l} \mathbf{1}_{n_l} \mathbf{1}_{n_l}^\top)^v (n_l \mu^{kl}(0) - \mathbf{1}_{n_l} \hat{W}_i(\theta^k + \delta u^k, \xi^k)), \end{aligned} \quad (54)$$

where the second equality used (53) and the third equality holds because $(C_0^l - \frac{1}{n_l} \mathbf{1}_{n_l} \mathbf{1}_{n_l}^\top) \mathbf{1}_{n_l} \mathbf{1}_{n_l}^\top \mu^{kl}(t) = 0$.

As a result, for any $v \in [0, T_c]$, we have

$$\begin{aligned} &\left\| \mathbb{E} [n_l \mu^{kl}(v)] - \mathbf{1}_{n_l} \hat{J}_i(\theta^k + \delta u^k) \right\| \\ &\leq \left\| \mathbb{E} [n_l \mu^{kl}(v) - \mathbf{1}_{n_l} \hat{W}_i(\theta^k + \delta u^k, \xi^k)] \right\| + \left\| \mathbf{1}_{n_l} \hat{J}_i(\theta^k + \delta u^k) - \mathbb{E} [\mathbf{1}_{n_l} \hat{W}_i(\theta^k + \delta u^k, \xi^k)] \right\| \\ &\leq \rho_l^v \left\| \mathbb{E} [n_l \mu^{kl}(0) - \mathbf{1}_{n_l} \hat{W}_i(\theta^k + \delta u^k, \xi^k)] \right\| + n_l^2 \gamma^{T_e} J_0 \\ &\leq \rho_l^v \left\| \mathbb{E} [n_l \mu^{kl}(0) - \mathbf{1}_{n_l} \hat{J}_i(\theta^k + \delta u^k)] \right\| + (\rho_l^v + 1) n_l^2 \gamma^{T_e} J_0 \\ &\leq \rho_l^v n_l^2 (J_u - J_l) + (\rho_l^v + 1) n_l^2 \gamma^{T_e} J_0 \\ &= \rho_l^v n_l^2 (J_u - J_l + \gamma^{T_e} J_0) + n_l^2 \gamma^{T_e} J_0, \end{aligned} \quad (55)$$

where the second inequality used (54) and Lemma 7, the third inequality used Lemma 7 again, and the last inequality used the uniform bound of J_i and the fact that $\mathbb{E}[\mu_i^{kl}(0)] = \mathbb{E}[W_i(\theta^k + \delta u^k, \xi^k)] \leq J_i^\delta(\theta^k)$.

Due to Assumption 4, we have $\min_{j \in \mathcal{I}_i^L} W_j(\theta^k + \delta u^k, \xi^k) \leq \mu_i^{kl}(T_c) \leq \max_{j \in \mathcal{I}_i^L} W_j(\theta^k + \delta u^k, \xi^k)$. Let $i_0 = \arg \max_{j \in \mathcal{I}_i^L} |W_j(\theta^k + \delta u^k, \xi^k)|$. Then we have

$$\begin{aligned} \mathbb{E}_{\xi^k \sim \mathcal{H}} \left[[n_l \mu_i^{kl}(T_c)]^2 \right] &\leq n_l^2 \mathbb{E}_{\xi^k \sim \mathcal{H}} [W_{i_0}^2(\theta^k + \delta u^k, \xi^k)] \\ &= n_l^2 \mathbb{E}_{\xi^k \sim \mathcal{H}} [(\xi_{i_0}^k)^2] + n_l^2 (\mathbb{E}_{\xi^k \sim \mathcal{H}} [W_{i_0}(\theta^k + \delta u^k, \xi^k)])^2 \\ &\leq n_l^2 \sigma_0^2 + n_l^2 (J_{i_0}(\theta^k + \delta u^k) + \gamma^{T_e} J_0)^2 \\ &\leq n_l^2 (\sigma_0^2 + (1 + \gamma^{T_e})^2 J_0^2). \end{aligned} \quad (56)$$

The proof is completed. \square

Proof of Lemma 9: According to (16), we have

$$\begin{aligned} \mathbb{E}[\|g_i(\theta^k, u^k, \xi^k)\|^2] &= \frac{1}{\delta^2} \mathbb{E}_{u_i^k} \left[\mathbb{E}_{\xi^k \sim \mathcal{H}} \left[(n_l \mu_i^{kl}(T_c))^2 \right] \|u_i^k\|^2 \right] \\ &\leq \frac{B_l^\mu}{\delta^2} \mathbb{E} [\|u_i^k\|^2] \\ &= \frac{B_l^\mu}{\delta^2 \varphi} \int_{\mathbb{R}^{d_i}} \|u_i^k\|^2 e^{-\frac{1}{2} \|u_i^k\|^2} du_i^k \int_{\mathbb{R}^{d-d_i}} e^{-\frac{1}{2} \|v\|^2} dv \\ &\leq \frac{B_l^\mu}{\delta^2 \varphi} d_i \int_{\mathbb{R}^{d_i}} e^{-\frac{1}{2} \|u_i^k\|^2} du_i^k \int_{\mathbb{R}^{d-d_i}} e^{-\frac{1}{2} \|v\|^2} dv \\ &= \frac{B_l^\mu d_i}{\delta^2}, \end{aligned} \quad (57)$$

where φ is defined in (45), the first inequality used (20), and the second inequality holds because $\int_{\mathbb{R}^{d_i}} \|u_i^k\|^2 e^{-\frac{1}{2} \|u_i^k\|^2} du_i^k \leq d_i \int_{\mathbb{R}^{d_i}} e^{-\frac{1}{2} \|u_i^k\|^2} du_i^k$, which has been proved in [38, Lemma 1]. \square

Proof of Theorem 1: Statement (i) is obtained by using the Lipschitz continuity of $J(\theta)$, which has been proved in [38].

Now we prove statement (ii). According to Assumption 2 and [38, Lemma 2], the gradient of $J^\delta(\theta)$ is \sqrt{dL}/r -Lipschitz continuous. Let $g(\theta^k) = (g_1^\top(\theta^k), \dots, g_N^\top(\theta^k))^\top \in \mathbb{R}^d$, the following holds:

$$|J^\delta(\theta^{k+1}) - J^\delta(\theta^k) - \langle \nabla_\theta J^\delta(\theta^k), \eta g(\theta^k) \rangle| \leq \frac{\sqrt{dL}}{2r} \eta^2 \|g(\theta^k, u^k, \xi^k)\|^2, \quad (58)$$

which implies that

$$\langle \nabla_\theta J^\delta(\theta^k), \eta g(\theta^k) \rangle \leq J^\delta(\theta^{k+1}) - J^\delta(\theta^k) + \frac{\sqrt{dL}}{2r} \eta^2 \|g(\theta^k, u^k, \xi^k)\|^2. \quad (59)$$

Lemma 9 implies that

$$\begin{aligned} \mathbb{E}[\|g(\theta^k, u^k, \xi^k)\|^2] &= \sum_{i=1}^N \mathbb{E}[\|g_i(\theta^k, u^k, \xi^k)\|^2] \\ &\leq \sum_{i=1}^N B_l^\mu d_i / \delta^2 \leq B_0^\mu d / \delta^2, \end{aligned} \quad (60)$$

where $B_0^\mu = \max_{l \in \mathcal{C}} B_l^\mu = n_0^2 (\sigma_0^2 + (1 + \gamma^{T_e})^2 J_0^2)$.

Moreover, Lemma 8 implies that

$$\begin{aligned} \mathbb{E} [\langle \nabla_{\theta_i} J^\delta(\theta^k), g_i(\theta^k, u^k, \xi^k) \rangle] &= \mathbb{E} [\|\nabla_{\theta_i} J^\delta(\theta^k)\|^2] + \mathbb{E} [\langle \nabla_{\theta_i} J^\delta(\theta^k), n_l \mu_i^{kl}(T_c) u_i^k / \delta - \hat{J}_i(\theta^k + \delta u^k) u_i^k / \delta \rangle] \\ &\geq \mathbb{E} [\|\nabla_{\theta_i} J(\theta^k)\|^2] - \frac{1}{2} \mathbb{E} [\|\nabla_{\theta_i} J(\theta^k)\|^2 + E_i^2 \|u_i^k\|^2 / \delta^2] \\ &= \frac{1}{2} \mathbb{E} [\|\nabla_{\theta_i} J(\theta^k)\|^2] - \frac{E_i^2 d_i}{2 \delta^2}, \end{aligned} \quad (61)$$

where the first equality used Lemma 2 and $\nabla_{\theta_i} \hat{J}^\delta(\theta^k) = \mathbb{E}[\hat{J}_i(\theta^k + \delta u^k) u_i^k / \delta]$, the inequality used (19). Summing (61) over i from 0 to N yields

$$\mathbb{E}[\langle \nabla_{\theta} J^\delta(\theta^k), g(\theta^k, u^k, \xi^k) \rangle] \geq \frac{1}{2} \mathbb{E}[\|\nabla_{\theta} J(\theta^k)\|^2] - \frac{E_0^2 d}{2\delta^2}, \quad (62)$$

where $E_0 = \max_{i \in \mathcal{V}} E_i$.

Combining (62) and (59), and taking expectation on both sides, we obtain

$$\begin{aligned} & \frac{1}{2} \eta \mathbb{E}[\|\nabla_{\theta} J^\delta(\theta^k)\|^2] - \eta \frac{E_0^2 d}{2\delta^2} \\ & \leq \mathbb{E}[J^\delta(\theta^{k+1}) - J^\delta(\theta^k)] + \frac{\sqrt{d}L}{2\delta} \eta^2 \mathbb{E}[\|g(\theta^k, u^k, \xi^k)\|^2] \\ & \leq \mathbb{E}[J^\delta(\theta^{k+1}) - J^\delta(\theta^k)] + \frac{LB_0^\mu d^{1.5}}{2\delta^3} \eta^2, \end{aligned} \quad (63)$$

where the second inequality employed (60).

Note that under the conditions on T_c , we have

$$E_0 \leq \frac{\epsilon^{1.5}}{\sqrt{2Ld}}. \quad (64)$$

Summing (63) over k from 0 to $K-1$ and dividing both sides by K , yields

$$\frac{1}{K} \sum_{k=0}^{K-1} \mathbb{E}[\|\nabla_{\theta} J^\delta(\theta^k)\|^2] \quad (65)$$

$$\leq \frac{2}{\eta} \left[\frac{1}{K} (\mathbb{E}[J^\delta(\theta^K)] - J^\delta(\theta^0)) + \frac{LB_0^\mu d^{1.5}}{2\delta^3} \eta^2 \right] + \frac{E_0^2 d}{\delta^2} \quad (66)$$

$$\leq \frac{2}{\eta} \left[\frac{1}{K} (NJ_u - J^\delta(\theta^0)) + B_0^\mu \frac{Ld^{1.5}}{2\delta^3} \eta^2 \right] + \frac{\epsilon}{2} \quad (67)$$

$$\leq \frac{d^{1.5}}{\epsilon^{1.5} \sqrt{K}} [2(NJ_u - J^\delta(\theta^0)) + L^4 B_0^\mu] + \frac{\epsilon}{2}, \quad (68)$$

where the second inequality used (64), the last inequality used the conditions on δ and η . The proof is completed. \square

Proof of Lemma 10: When $\kappa \geq D_l^*$, (25) implies $\tilde{J}_i^\delta(\theta) = \hat{J}_i^\delta(\theta)$. By Lemma 2, $\|\nabla_{\theta_i} \tilde{J}_i^\delta(\theta) - \nabla_{\theta_i} J^\delta(\theta)\| = 0$. Next we analyze the other case.

Let $r_i^\theta(s_i(t), a_i(t))$ be the individual reward of agent i at time t under the global policy $\pi(\theta)$. Due to Lemma 2, it suffices to analyze $\|\nabla_{\theta_i} \tilde{J}_i^\delta - \nabla_{\theta_i} \hat{J}_i^\delta\|$.

Let $J_{i,\kappa}^\delta(\theta) = \sum_{j \in \bar{\mathcal{V}}_l^\kappa} \sum_{t=0}^\kappa \gamma^t r_j(t)(s_j(t), a_j(t))$, and $\bar{J}_{i,\kappa}^\delta(\theta) = \sum_{j \in \bar{\mathcal{V}}_l^\kappa} \sum_{t=\kappa+1}^\infty \gamma^t r_j(t)(s_j(t), a_j(t))$. Then

$$\tilde{J}_i^\delta(\theta) - \hat{J}_i^\delta(\theta) = J_{i,\kappa}^\delta(\theta) + \bar{J}_{i,\kappa}^\delta(\theta). \quad (69)$$

Notice that if $D(\mathcal{V}_l, j) > \kappa$, then the reward of each agent $j \in \bar{\mathcal{V}}_l^\kappa$ is not affected by cluster \mathcal{V}_l at any time

step $t \leq \kappa$. Therefore, $\nabla_{\theta_i} J_{i,\kappa}^\delta(\theta) = 0$. It follows that

$$\begin{aligned}
& \|\nabla_{\theta_i} \tilde{J}_i^\delta(\theta) - \nabla_{\theta_i} \hat{J}_i^\delta(\theta)\| = \|\nabla_{\theta_i} \bar{J}_{i,\kappa}^\delta(\theta)\| \\
&= \left\| \mathbb{E} \left[\sum_{j \in \bar{\mathcal{V}}_i^\kappa} \frac{\sum_{t=\kappa+1}^{\infty} \gamma^t r_j^{\theta+\delta u}(s_j(t), a_j(t)) - \sum_{t=\kappa+1}^{\infty} \gamma^t r_j^\theta(s_j(t), a_j(t))}{\delta} u_i \right] \right\| \\
&\leq \sum_{j \in \bar{\mathcal{V}}_i^\kappa} \mathbb{E}_{u \sim \mathcal{N}(0, I_d)} \left[\left\| \mathbb{E}_{s \sim \mathcal{D}} \sum_{t=\kappa+1}^{\infty} \gamma^t \frac{r_j^{\theta+\delta u}(s_j(t), a_j(t)) - r_j^\theta(s_j(t), a_j(t))}{\delta} u_i \middle| s_0 = s \right\| \right] \\
&= \gamma^{\kappa+1} \sum_{j \in \bar{\mathcal{V}}_i^\kappa} \mathbb{E}_{u \sim \mathcal{N}(0, I_d)} \left[\left\| \mathbb{E}_{s \sim \mathcal{D}} \left[\frac{V_j^{\pi(\theta+\delta u)}(s_{j,\kappa+1}) - V_j^{\pi(\theta)}(s_{j,\kappa+1})}{\delta} u_i \middle| s_0 = s \right] \right\| \right] \quad (70) \\
&\leq \gamma^{\kappa+1} \sum_{j \in \bar{\mathcal{V}}_i^\kappa} L_j \mathbb{E}[\|u\| \|u_i\|] \\
&\leq \gamma^{\kappa+1} \sum_{j \in \bar{\mathcal{V}}_i^\kappa} L_j (\mathbb{E}[\|u\|^2])^{1/2} (\mathbb{E}[\|u_i\|^2])^{1/2} \\
&\leq \gamma^{\kappa+1} \sum_{j \in \bar{\mathcal{V}}_i^\kappa} L_j \sqrt{dd_i},
\end{aligned}$$

where the second equality used the two-point feedback zeroth-order oracle [38], the third equality used the definition of $V_i^{\pi(\theta)}(s)$, the second inequality used Assumption 2, the third inequality used Holder's inequality. The proof is completed. \square

Proof of Theorem 2: Here we only show the different part compared with the proof of Theorem 1.

$$\begin{aligned}
& \mathbb{E}[\langle \nabla_{\theta_i} J^\delta(\theta^k), g_i(\theta^k, u^k, \xi^k) \rangle] = \mathbb{E}[\|\nabla_{\theta_i} J^\delta(\theta^k)\|^2] \\
&+ \mathbb{E}[\langle \nabla_{\theta_i} J^\delta(\theta^k), n_l \mu_i^{kl}(T_c) u_i^k / \delta - \tilde{J}_i(\theta^k + \delta u^k) u_i^k / \delta \rangle] + \mathbb{E}[\langle \nabla_{\theta_i} J^\delta(\theta^k), \nabla_{\theta_i} \tilde{J}_i(\theta^k) - \nabla_{\theta_i} \hat{J}_i(\theta^k) \rangle] \\
&\geq \mathbb{E}[\|\nabla_{\theta_i} J(\theta^k)\|^2] - \frac{1}{2} \mathbb{E}[\|\nabla_{\theta_i} J(\theta^k)\|^2] - (E_i^\kappa)^2 \|u_i^k\|^2 / \delta^2 - \frac{d_i}{\delta^2} A_i^2 \quad (71) \\
&= \frac{1}{2} \mathbb{E}[\|\nabla_{\theta_i} J(\theta^k)\|^2] - \frac{(E_i^\kappa)^2 d_i}{\delta^2} - \frac{d_i}{\delta^2} A_i^2,
\end{aligned}$$

where $A_i = \gamma^{\kappa+1} \sum_{j \in \bar{\mathcal{V}}_i^\kappa} L_j \sqrt{dd_i}$, the first equality used $\mathbb{E}_{u_i^k}[\tilde{J}_i(\theta^k + \delta u^k) u_i^k / \delta] = \nabla_{\theta_i} \tilde{J}_i(\theta^k)$ and $\mathbb{E}_{u_i^k}[\hat{J}_i(\theta^k + \delta u^k) u_i^k / \delta] = \nabla_{\theta_i} \hat{J}_i(\theta^k)$, the inequality used $ab \geq -\frac{1}{4}a^2 - b^2$. Then we have

$$\mathbb{E}[\langle \nabla_{\theta} J^\delta(\theta^k), g(\theta^k, u^k, \xi^k) \rangle] \geq \frac{1}{2} \mathbb{E}[\|\nabla_{\theta} J(\theta^k)\|^2] - \frac{(E_0^\kappa)^2 d}{\delta^2} - \frac{d}{\delta^2} A_0^2, \quad (72)$$

where $E_0^\kappa = \max_{i \in \mathcal{V}} E_i^\kappa$, $A_0 = \max_{i \in \mathcal{V}} A_i = \gamma^{\kappa+1} \max_{l \in \mathcal{C}} |\bar{\mathcal{V}}_l^\kappa| L_0 \sqrt{dd_0}$.

It follows that

$$\begin{aligned}
& \frac{1}{2} \eta \mathbb{E}[\|\nabla_{\theta} J^\delta(\theta^k)\|^2] - \eta \frac{(E_0^\kappa)^2 d}{2\delta^2} - \frac{d}{\delta^2} A_0^2 \\
&\leq \mathbb{E}[J^\delta(\theta^{k+1}) - J^\delta(\theta^k)] + \frac{\sqrt{d} L}{2\delta} \eta^2 \mathbb{E}[\|g(\theta^k, u^k, \xi^k)\|^2] \quad (73) \\
&\leq \mathbb{E}[J^\delta(\theta^{k+1}) - J^\delta(\theta^k)] + \frac{L B_0^\kappa d^{1.5}}{2\delta^3} \eta^2,
\end{aligned}$$

where $B_0^\kappa = (n_l^\kappa)^2 (\sigma_0^2 + J_0^2)$.

Therefore, the following holds:

$$\begin{aligned}
& \frac{1}{K} \sum_{k=0}^{K-1} \mathbb{E}[\|\nabla_{\theta} J^{\delta}(\theta^k)\|^2] \\
& \leq \frac{2}{\eta} \left[\frac{1}{K} (\mathbb{E}[J^{\delta}(\theta^K)] - J^{\delta}(\theta^0)) + \frac{LB_0^{\kappa} d^{1.5}}{2\delta^3} \eta^2 \right] + \frac{2E_0^2 d}{\delta^2} + \frac{2d}{\delta^2} A_0^2 \\
& \leq \frac{2}{\eta} \left[\frac{1}{K} (NJ_u - J^{\delta}(\theta^0)) + (n_l^{\kappa})^2 (\sigma_0^2 + J_0^2) \frac{Ld^{1.5}}{2\delta^3} \eta^2 \right] + \frac{\epsilon}{2} + \frac{2d}{\delta^2} A_0^2 \\
& \leq \frac{d^{1.5}}{\epsilon^{1.5} \sqrt{K}} [2(NJ_u - J^{\delta}(\theta^0)) + (n_l^{\kappa})^2 (\sigma_0^2 + J_0^2) L^4] + \frac{\epsilon}{2} + \frac{2d}{\delta^2} A_0^2.
\end{aligned} \tag{74}$$

The proof is completed. \square

References

- [1] R. S. Sutton and A. G. Barto, *Reinforcement learning: An introduction*. MIT press, 2018.
- [2] D. Silver, J. Schrittwieser, K. Simonyan, I. Antonoglou, A. Huang, A. Guez, T. Hubert, L. Baker, M. Lai, A. Bolton *et al.*, “Mastering the game of go without human knowledge,” *nature*, vol. 550, no. 7676, pp. 354–359, 2017.
- [3] A. S. Polydoros and L. Nalpantidis, “Survey of model-based reinforcement learning: Applications on robotics,” *Journal of Intelligent & Robotic Systems*, vol. 86, no. 2, pp. 153–173, 2017.
- [4] S. Mukherjee, A. Chakrabortty, H. Bai, A. Darvishi, and B. Fardanesh, “Scalable designs for reinforcement learning-based wide-area damping control,” *IEEE Transactions on Smart Grid*, vol. 12, no. 3, pp. 2389–2401, 2021.
- [5] S. Kar, J. M. Moura, and H. V. Poor, “ $Q\mathcal{D}$ -learning: A collaborative distributed strategy for multi-agent reinforcement learning through consensus + innovations,” *IEEE Transactions on Signal Processing*, vol. 61, no. 7, pp. 1848–1862, 2013.
- [6] S. Omidshafiei, J. Pazis, C. Amato, J. P. How, and J. Vian, “Deep decentralized multi-task multi-agent reinforcement learning under partial observability,” in *International Conference on Machine Learning*. PMLR, 2017, pp. 2681–2690.
- [7] R. Lowe, Y. Wu, A. Tamar, J. Harb, P. Abbeel, and I. Mordatch, “Multi-agent actor-critic for mixed cooperative-competitive environments,” *arXiv preprint arXiv:1706.02275*, 2017.
- [8] K. Zhang, Z. Yang, H. Liu, T. Zhang, and T. Basar, “Fully decentralized multi-agent reinforcement learning with networked agents,” in *International Conference on Machine Learning*. PMLR, 2018, pp. 5872–5881.
- [9] A. OroojlooyJadid and D. Hajinezhad, “A review of cooperative multi-agent deep reinforcement learning,” *arXiv preprint arXiv:1908.03963*, 2019.
- [10] Y. Zhang and M. M. Zavlanos, “Cooperative multi-agent reinforcement learning with partial observations,” *arXiv preprint arXiv:2006.10822*, 2020.
- [11] T. Chen, K. Zhang, G. B. Giannakis, and T. Basar, “Communication-efficient policy gradient methods for distributed reinforcement learning,” *IEEE Transactions on Control of Network Systems*, 2021.

- [12] L. Cassano, K. Yuan, and A. H. Sayed, “Multiagent fully decentralized value function learning with linear convergence rates,” *IEEE Transactions on Automatic Control*, vol. 66, no. 4, pp. 1497–1512, 2020.
- [13] S. Gronauer and K. Diepold, “Multi-agent deep reinforcement learning: a survey,” *Artificial Intelligence Review*, pp. 1–49, 2021.
- [14] G. Qu, A. Wierman, and N. Li, “Scalable reinforcement learning of localized policies for multi-agent networked systems,” in *Learning for Dynamics and Control*. PMLR, 2020, pp. 256–266.
- [15] G. Qu, Y. Lin, A. Wierman, and N. Li, “Scalable multi-agent reinforcement learning for networked systems with average reward,” *Advances in Neural Information Processing Systems*, vol. 33, 2020.
- [16] Y. Lin, G. Qu, L. Huang, and A. Wierman, “Multi-agent reinforcement learning in stochastic networked systems,” in *Thirty-Fifth Conference on Neural Information Processing Systems*, 2021.
- [17] K. Zhang, Z. Yang, and T. Başar, “Multi-agent reinforcement learning: A selective overview of theories and algorithms,” *Handbook of Reinforcement Learning and Control*, pp. 321–384, 2021.
- [18] C. Guestrin, M. Lagoudakis, and R. Parr, “Coordinated reinforcement learning,” in *ICML*, vol. 2. Citeseer, 2002, pp. 227–234.
- [19] J. R. Kok and N. Vlassis, “Collaborative multiagent reinforcement learning by payoff propagation,” *Journal of Machine Learning Research*, vol. 7, pp. 1789–1828, 2006.
- [20] G. Jing, H. Bai, J. George, A. Chakrabortty, and P. K. Sharma, “Asynchronous distributed reinforcement learning for LQR control via zeroth-order block coordinate descent,” *arXiv preprint arXiv:2107.12416*, 2021.
- [21] D. Görges, “Distributed adaptive linear quadratic control using distributed reinforcement learning,” *IFAC-PapersOnLine*, vol. 52, no. 11, pp. 218–223, 2019.
- [22] Y. Li, Y. Tang, R. Zhang, and N. Li, “Distributed reinforcement learning for decentralized linear quadratic control: A derivative-free policy optimization approach,” *IEEE Transactions on Automatic Control*, 2021.
- [23] G. Jing, H. Bai, J. George, and A. Chakrabortty, “Model-free optimal control of linear multi-agent systems via decomposition and hierarchical approximation,” *IEEE Transactions on Control of Network Systems*, 2021.
- [24] M. L. Littman, “Markov games as a framework for multi-agent reinforcement learning,” in *Machine learning proceedings*. Elsevier, 1994, pp. 157–163.
- [25] S. V. Macua, A. Tukiainen, D. G.-O. Hernández, D. Baldazo, E. M. de Cote, and S. Zazo, “Diff-dac: Distributed actor-critic for average multitask deep reinforcement learning,” in *Adaptive Learning Agents (ALA) Conference*, 2018.
- [26] A. Olshevsky, “Linear time average consensus on fixed graphs and implications for decentralized optimization and multi-agent control,” *arXiv preprint arXiv:1411.4186*, 2014.
- [27] G. Jing, H. Bai, J. George, A. Chakrabortty, P. Sharma *et al.*, “Distributed cooperative multi-agent reinforcement learning with directed coordination graph,” *arXiv preprint arXiv:2201.04962*, 2022.
- [28] A. Vemula, W. Sun, and J. Bagnell, “Contrasting exploration in parameter and action space: A zeroth-order optimization perspective,” in *The 22nd International Conference on Artificial Intelligence and Statistics*. PMLR, 2019, pp. 2926–2935.

- [29] H. Kumar, D. S. Kalogerias, G. J. Pappas, and A. Ribeiro, “Zeroth-order deterministic policy gradient,” *arXiv preprint arXiv:2006.07314*, 2020.
- [30] D. Hajinezhad, M. Hong, and A. Garcia, “Zone: Zeroth-order nonconvex multiagent optimization over networks,” *IEEE Transactions on Automatic Control*, vol. 64, no. 10, pp. 3995–4010, 2019.
- [31] C. Gratton, N. K. Venkategowda, R. Arablouei, and S. Werner, “Privacy-preserving distributed zeroth-order optimization,” *arXiv preprint arXiv:2008.13468*, 2020.
- [32] Y. Tang, J. Zhang, and N. Li, “Distributed zero-order algorithms for nonconvex multi-agent optimization,” *IEEE Transactions on Control of Network Systems*, 2020.
- [33] A. Akhavan, M. Pontil, and A. B. Tsybakov, “Distributed zero-order optimization under adversarial noise,” *arXiv preprint arXiv:2102.01121*, 2021.
- [34] Y. Tang, Z. Ren, and N. Li, “Zeroth-order feedback optimization for cooperative multi-agent systems,” *arXiv preprint arXiv:2011.09728*, 2020.
- [35] G. Jing, H. Bai, J. George, A. Chakrabortty, and P. K. Sharma, “Learning distributed stabilizing controllers for multi-agent systems,” *IEEE Control Systems Letters*, 2021.
- [36] P. Sunehag, G. Lever, A. Gruslys, W. M. Czarnecki, V. Zambaldi, M. Jaderberg, M. Lanctot, N. Sonnerat, J. Z. Leibo, K. Tuyls *et al.*, “Value-decomposition networks for cooperative multi-agent learning,” *arXiv preprint arXiv:1706.05296*, 2017.
- [37] T. Zhang, Y. Li, C. Wang, G. Xie, and Z. Lu, “Fop: Factorizing optimal joint policy of maximum-entropy multi-agent reinforcement learning,” in *International Conference on Machine Learning*. PMLR, 2021, pp. 12 491–12 500.
- [38] Y. Nesterov and V. Spokoiny, “Random gradient-free minimization of convex functions,” *Foundations of Computational Mathematics*, vol. 17, no. 2, pp. 527–566, 2017.
- [39] L. Xiao and S. Boyd, “Fast linear iterations for distributed averaging,” *Systems & Control Letters*, vol. 53, no. 1, pp. 65–78, 2004.
- [40] Y. Zhang, Y. Zhou, K. Ji, and M. M. Zavlanos, “A new one-point residual-feedback oracle for black-box learning and control,” *Automatica*, p. 110006, 2021.
- [41] L. Xiao, S. Boyd, and S. Lall, “A scheme for robust distributed sensor fusion based on average consensus,” in *IPSN 2005. Fourth International Symposium on Information Processing in Sensor Networks, 2005*. IEEE, 2005, pp. 63–70.